Hindawi
Science and Technology of Nuclear Installations
Volume 2022, Article ID 2755471, 22 pages
https://doi.org/10.1155/2022/2755471

Review Article

Debris Bed Self-Leveling Mechanism and Characteristics for Core Disruptive Accident of Sodium-Cooled Fast Reactor: Review of Experimental and Modeling Investigations

Ruicong Xu and Songbai Cheng

Sino-French Institute of Nuclear Engineering and Technology, Sun Yat-Sen University, Tang-Jia-Wan, Zhuhai 519-082, Guangdong, China

Correspondence should be addressed to Songbai Cheng; chengsb3@mail.sysu.edu.cn

Received 3 April 2022; Revised 3 July 2022; Accepted 15 July 2022; Published 22 August 2022

Academic Editor: Leon Cizelj

Evaluations of the Core Disruptive Accident (CDA) are significantly important for safety analysis of Sodium-cooled Fast Reactor (SFR) despite the very low probability of occurrence for CDA. During the material-relocation phase in CDA of SFR, the molten materials are possibly released from the core region into subcooled sodium, subsequently forming the debris bed on the lower part of the reactor vessel after being quenched and fragmented. The accumulated high-temperature debris with decay heat can cause sodium coolant boiling, leading to the so-called "debris bed self-leveling behavior" during which the shape of the debris bed becomes flattered (leveling). It is important to investigate the debris bed self-leveling behavior due to its potential capacity to induce the transfer of debris and affect the ability of cooling and criticality of the debris bed. Thus, in recent years, valuable knowledge concerning the mechanism and characteristics of this behavior was accumulated through lots of experimental results and modeling developments. Aimed at providing a valuable guideline for future investigations on this issue, in this study, the past experimental and modeling investigations on debris bed self-leveling mechanism and characteristics are systematically summarized and reviewed, and some future remarks are also proposed to promote the progression of further research for SFR severe accident analysis.

1. Introduction

The Sodium-cooled Fast Reactor (SFR) is one of the most promising Generation-IV nuclear reactor systems [1–3]. However, safety is an unavoidable issue that restricts the development of SFR [4, 5]. Considering the fact that the most neutronically reactive configuration is not achieved for intact SFR core due to its specific design [6, 7], evaluation of Core Disruptive Accidents (CDAs) is regarded as an essential topic for SFR safety analysis despite their extremely low probability of occurrence. During a postulated CDA in SFR, the molten fuel, molten structures, and other materials are possible to be discharged and released from the core area to the subcooled sodium pool [8, 9]. Subsequently, as shown in Figure 1, along with the fast quenching and fragmentation, the molten materials will become solid debris and accumulate on the core-support structure in the lower part of the reactor vessel to form the debris bed [10, 11]. To achieve In-Vessel Retention (IVR), which is primely essential for SFR, it is necessary to ensure the adequate cooling of the debris beds and their neutronically subcritical configuration [12, 13]. Nevertheless, it was recognized that the sodium coolant is probably heated and boiled by the high-temperature accumulated debris with decay heat, causing the interactions between bubbles and solid debris within debris beds [10, 14]. As illustrated in Figure 2, due to the sodium boiling, the shape of debris beds might gradually vary from a convex one to a leveling one (namely, debris bed self-leveling behavior) within tens of seconds to hundreds of seconds, thereby possibly inducing the transfer of fuel debris (for instance, in the multi-layer core catcher) [15]. Through the debris bed, self-leveling progression and transfer of fuel

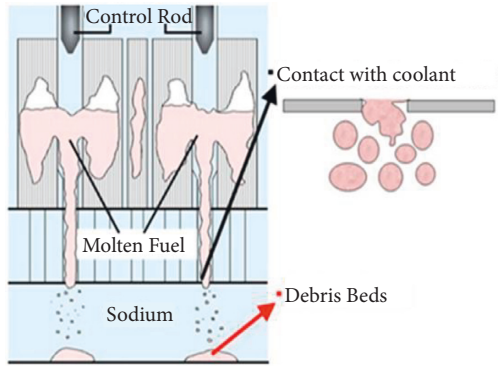

Figure 1: The formation of debris bed.

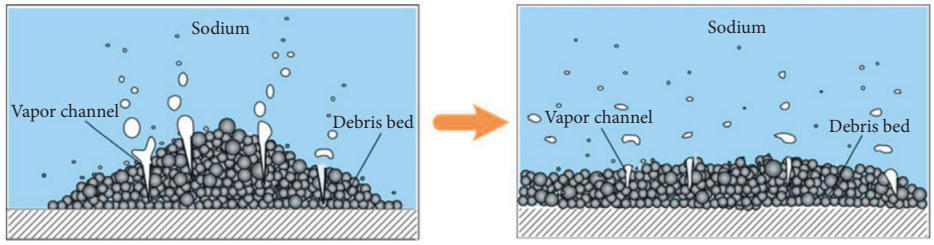

Figure 2: Debris bed self-leveling behavior.

debris, the heights of debris beds are expected to be suppressed below the coolable limit to avoid the potential debris remelting [15].

Recognizing the importance of the self-leveling behavior in heat-removal capability, Hesson et al. (1971) and Gabor (1974) conducted several pioneering experiments separately [16, 17]. In their experiments, through the respective introduction of airflow into a particle bed and volume-heating of a UO_2-salt particle bed in water, the self-leveling behavior was confirmed to exist. Further, it was experimentally validated that even with a low boiling intensity; the debris bed self-leveling behavior could be found easily [18]. However, in these pioneering experiments, the self-leveling mechanism and characteristics were not clearly and detailly illuminated due to the relatively limited experimental conditions considered and data acquired.

On the other hand, it should also be pointed out that the debris bed self-leveling behavior with its spreading was also found and widely investigated in the context of Light Water Reactor (LWR) severe accidents after the earliest confirmation of the existence of this behavior in CDA of SFR, and the findings and knowledge from these works also contributed to the understandings of such behavior [19–28]. However, different from the SFR, in the case of LWR, the debris bed was formed with an overall several-millimeter debris size in a deep water pool under the reactor vessel (i.e., ex-vessel) over the containment basemat, and attention was generally paid to its ability of cooling and the Molten Core–Concrete Interaction (MCCI) for assessing the response of containment [19–28]. While regarding the SFR, the debris size is more widely ranged (e.g., from 0.1 millimeters to several millimeters) [11, 29], and the aim of studying the self-leveling behavior is to improve the structural designs for the SFR safety devices to ensure IVR (such as core catcher) in case of CDAs with the considerations of not only the ability of cooling of debris bed but also its subcritical neutronic configuration. Nevertheless, thanks to the evaluations of debris bed ability of cooling in the studies for LWR severe accidents, it was understood that the heat-removal capability of debris beds is remarkably dependent on their geometries (such as shapes and heights) [19–23], thereby enlightening the investigations on clarifying the debris bed self-leveling mechanism and characteristics (e.g., leveling tendency and velocity) for SFR, which is of great essence for the improved design of in-vessel safety devices.

To elucidate the debris bed self-leveling mechanism for better comprehending the CDA of SFR, over the past dozen years, by using solid particle beds and water to respectively simulate the debris beds and liquid sodium, lots of experimental studies were elaborately performed by assuming an initial conical (or convex) shape of debris bed. Overall, Figure 3 summarizes these experiments, which can be categorized into two parts: microscopic flow regime and macroscopic self-leveling experiments. To simulate the sodium boiling condition as a result of the decay heat generated from accumulated debris, the depressurization boiling method was initially applied at Kyushu University and Japan Atomic Energy Agency (JAEA) to ensure an axial increment of void distribution within particle beds [10, 14]. Further, a series of experiments was carried out by applying the bottom-heated boiling method to examine the reliability of the depressurization method [10]. Based on the experimental observations, the general characteristics of self-leveling behavior and some parametric effects (e.g., boiling intensity, particle size/density) on the leveling onset and

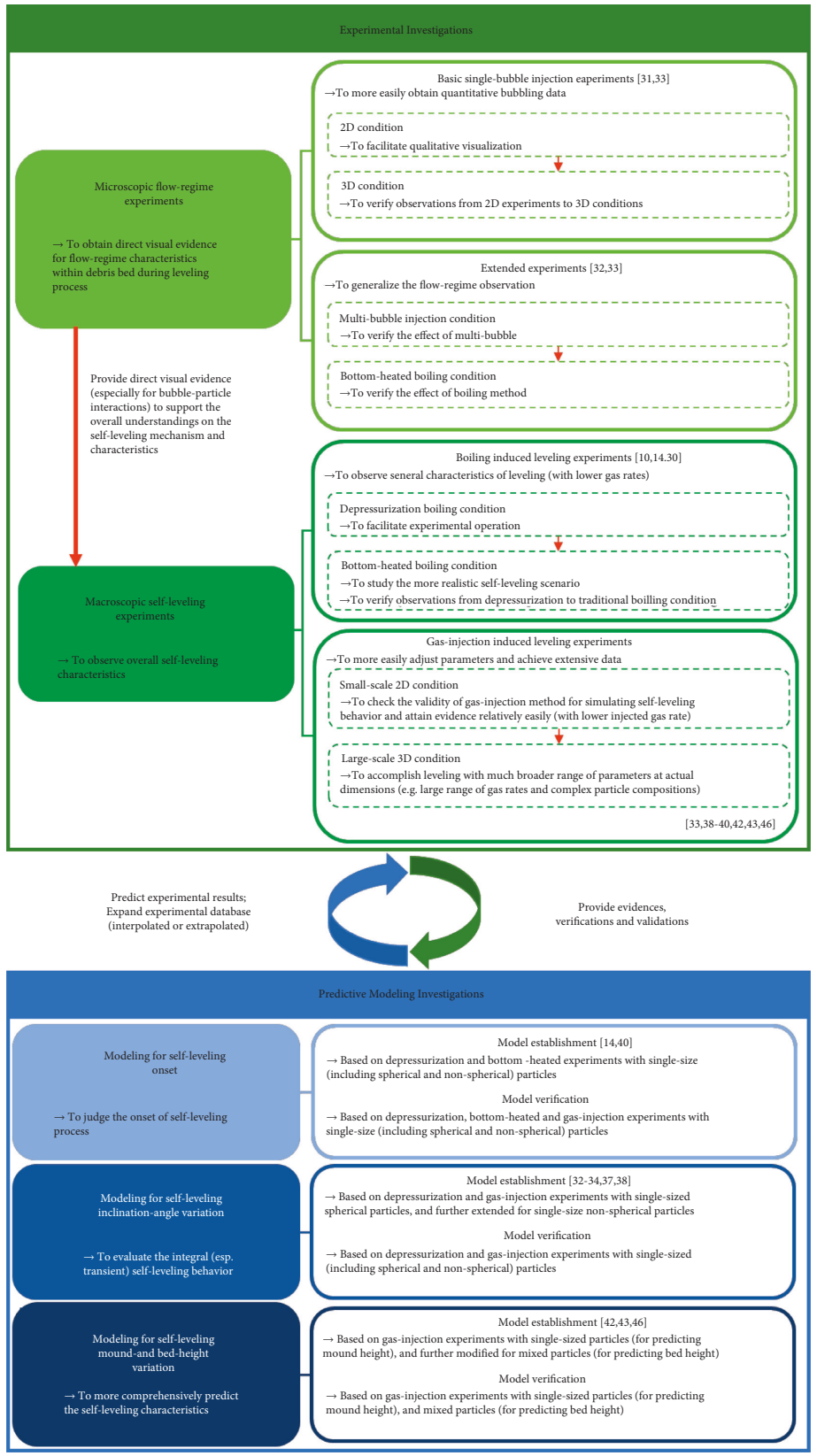

Figure 3: Summary of past experimental and modeling studies.

progression, were identified. In addition, several bottom-heated experiments carried out at Indira Gandhi Centre for Atomic Research (IGCAR) further validated the occurrence of self-leveling under low heat fluxes (lower than the dry-out heat flux) and the imperfect horizontally level-off for large-density particles [30]. However, due to the lack of sufficient visualization evidence, the self-leveling mechanism was still needed to be more comprehensively illuminated. Hence, through the microscopic flow regime experiments by employing various bubbling approaches (as summarized in Figure 3) [31–33], the bubble flow characteristics within the particle beds were ascertained, thereby effectively deepening the understanding of the observed overall self-leveling characteristics.

Nevertheless, to attain more valuable results through experiments supporting the predictive modeling development, the applicability of the gas-injection method, by which the adjustment and controlled behavior of the gas phase were able to be more expediently realized, was examined by a series of macroscopic quasi-two-dimensional (2D) small-scale experiments for self-leveling behaviors with single-size spherical particles [33]. Then, the gas-injection method was further employed in the three-dimensional (3D) large-scale self-leveling experiments at Kyushu University, JAEA, and Xi'an Jiao Tong University to diminish the wall effect as well as extend the parametric range (e.g., gas flow rate) for extrapolating the experimental data and findings [32–40]. However, recognizing that the debris beds are probably composed of solid fragments and particles with varying sizes and porosities in the hypothetical CDAs of SFR through the interaction between melt and coolant [11, 41], various particle components, such as single-size non-spherical particles as well as mixed particles (i.e., mixed-density, mixed-size, and mixed-shape particles), were subsequently applied to form the particle beds for the large-scale macroscopic self-leveling experiments [38–40, 42, 43].

Considering the complexity and uncertainty of the multiphase flow phenomena occurring in the debris bed self-leveling process [14, 34], aside from experimental investigations, modeling investigations were also paid attention to because the modeling approach can not only attractively and reasonably expand (interpolate or extrapolate) the experimental findings and data with much lower cost, but also accumulate valuable knowledge for improving and verifying the computer models involved in numerical simulations [44, 45]. Noticing this point, motivated to predict the self-leveling onset, according to the self-leveling experimental studies using depressurization methods, a semi-empirical model was proposed [14], and further validated under gas-injection conditions [40]. However, in this predictive model, many assumptions should be adopted, especially for the one in that the topmost particle shifting represents the onset of the whole self-leveling process, during which lots of interactions within the particle beds should be considered for better evaluating the transient self-leveling behavior. Therefore, aimed at providing more comprehensive information for assessing the self-leveling development, a new predictive model for evaluating the variation of the inclination angles of the particle beds was empirically developed in accordance with the macroscopic self-leveling experiments using single-size spherical particles for depressurization and gas-injection cases [32–34, 37]. Then, through the introduction of a correlation factor estimating the particle-shape effect, the applicable range of this model was further expanded for non-spherical particles [38], so that the extensibility of this model for covering more complicated and more realistic conditions was revealed. While noticing the fact that the particle mound/bed height is also an important factor for the ability of cooling assessment of debris bed, the establishment of another predictive model focusing on the variation of the particle mound height was attempted for single-size particle (including spherical and non-spherical) cases to attain more useful understandings on the self-leveling development [46]. However, since it was further confirmed that the mixed-size particle characteristics could play a remarkable role in the progression of the self-leveling process, a predictive model for the variation of the particle bed height was subsequently proposed for being applicable in single-size and mixed-size particle cases [42, 43].

Noticing that understanding the debris bed self-leveling mechanism and characteristics are of great importance for the improvement of SFR safety assessment, this study carries out a systematic review and discussion of the relevant experimental and modeling investigations in the past dozen years on reveling the self-leveling mechanism and characteristics for SFR. Knowledge and understandings attained through experimental observations and model predictions regarding the debris bed self-leveling behavior are believed to be valuable for improving and verifying the computer models for SFR severe accident analysis [45], and optimizing the structural design of the core catcher of SFR. In this study, the experimental investigations are introduced and summarized in Section 2. In Section 3, the modeling developments and validations are described and discussed. Moreover, aimed at providing valuable references and guidance for future research on the debris bed self-leveling behavior, conclusions and some future prospects are also discussed in Section 4 and Section 5, respectively.

2. Experimental Investigations

2.1. Microscopic Flow Regime Behaviors

2.1.1. Experimental Conditions. Aiming at providing valuable results for understanding the self-leveling characteristics, in the experimental studies on microscopic flow regime behaviors, the gas-injection method with single bubble and multi bubbles and the bottom-heated boiling method were employed for 2D and 3D experimental systems (see Figure 4) to clarify the particle-bubble and particle-particle interactions within the particle beds. In the experiments, the particle beds with different heights were initially flat, and the particle properties (such as density and size) were also taken into account as important parameters, as listed in Table 1. Relative low gas flow rates (e.g., 1.7×10^{-3} and 2.7×10^{-3} L/min) were applied in the experiments with single-bubble injection by considering the early stages of sodium boiling inside the accumulated debris bed in a CDA of SFR [31]. On the other hand, in the bottom-heated experiments, water in the pool should be heated around its boiling point in advance.

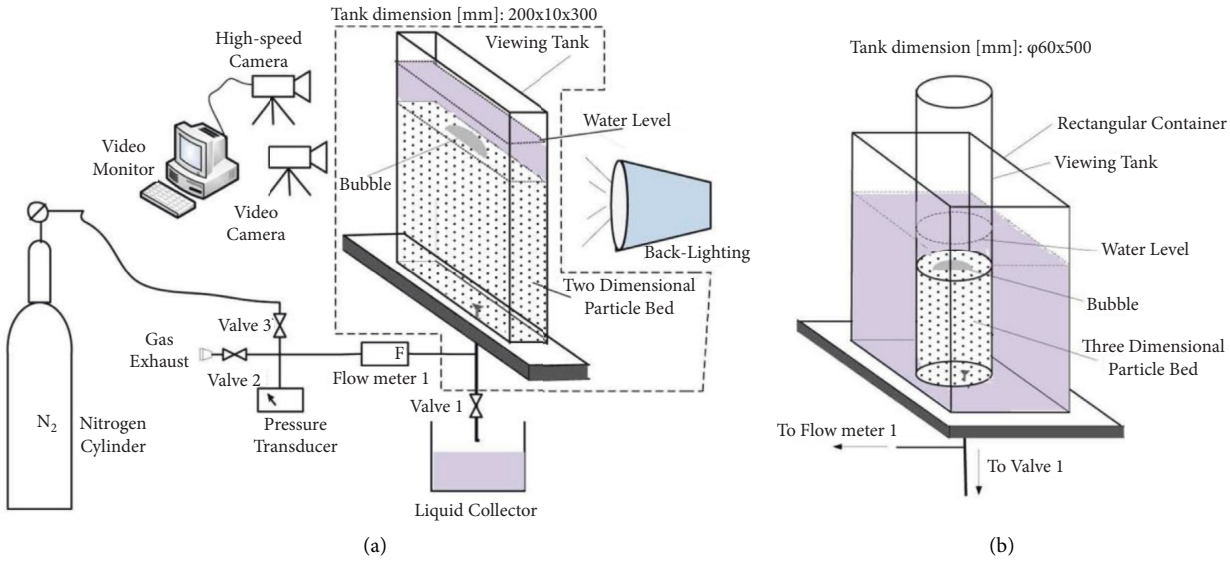

Figure 4: Experimental systems for microscopic flow regime studies with single-bubble injection [31] (a) 2D setup, (b) 3D setup.

2.1.2. Experimental Results. As displayed in Figure 5, it was found that there were three major flow regimes (i.e., bubble behaviors), namely the bubble coalescing regime, the transitional regime, and the bubble trapping regime, which existed as a result of the different bubble-particle interaction mechanism. Figure 6 further illustrates the flow-regime characteristics for single-bubble injections. To attain more comprehensive understanding of the characteristics of the injected bubble inside the particle beds, the parametric effects were also quantitatively investigated.

Figure 7 shows the influence of particle size (i.e., diameter) on the bubble frequency and bubble size at the surface of the particle bed. According to Figure 7(a), it is observable that the bubble frequency would first increase when particle size increased until a critical diameter of particle (near 1 mm) was achieved, and subsequently decrease. This can be explained by the reason that in the case of smaller particles (e.g., 0.4 mm), the bubble movements were restricted and hindered to some extent due to the compactly packed particle beds (i.e., particle beds with higher solid holdup). In addition, for small particles being light, it was easier to be suspended by upward rising bubbles, thereby providing a resistance to the rising bubbles due to their gravity [31]. Nevertheless, as particles enlarged, the particles become heavier and more difficult to be affected by these buoyancy effects; after particle size became sufficient large (e.g., ≥2 mm), bubbles would be trapped more and more significantly as a result of heavier particle weight, leading to lower surface bubble frequency. On the other hand, from Figure 7(b), it can be found that for the 2D system, the surface bubble size tended to decrease first until the particle diameters reached about 2 mm, and then increase up to particle diameters of nearly 4 mm, where the bubble size stabilized or trailed off. This might be explained by the reason that the bubble size was greatly influenced by the bubble coalescences in the bubble coalescing regime. Nevertheless, when particle size increased from 0.4 mm to 2 mm, this effect became less significant. Beyond 2 mm, the bubble trapping was more and more obvious, and hence the surface bubble size was found to increase due to the coalescence of trapped bubbles within the particle bed. However, if particle diameters became greater than 4 mm, quenching of the bubble trapping might cause no significant differences inside the particle bed [31].

One more significant point can be understood from Figure 7 is that for the cases with different particle bed heights and experimental dimensions (2D or 3D), the effect of particle size on the flow regime transitions could be found to be similar, although the wall effect manifested itself in a totally different manner in both systems. This indicates that the observed bubble behaviors should be the general characteristics, although the critical particle sizes required for attaining the regime transitions are quite different for 2D and 3D systems due to the extra degree of freedom in the 3D system, which would lead to the increase of bubble trails with particle size for the same bed height. This point has been also confirmed when different types of particles (with particle density ranging from 2.6 to 6.0 g/cm^3) were used [31].

Regarding the effect of particle density, it was also found that in the bubble coalescing regime, the surface frequency would be greater with the larger particle density due to less buoyant particles, causing less obstruction to bubble movement. While the tendency for surface bubble size was reversed because of the lessening possibility of bubble coalescence due to less buoyant particles caused by larger particle weight as particle density increased [31]. On the other hand, in the transitional regime, the effect of particle density on surface frequency seemed to be not significant because particles were heavy enough to cause a less buoyant effect from rising bubbles but still too small to trap the bubbles. While the surface bubble size was observed to be larger for cases with smaller particle density for the reason that higher-density particles might lead to bubble fragmentation rather than bubble coalescence [31]. Further, for the bubble trapping regime, the larger the particle density was, the smaller the surface bubble frequency and size were

Table 1: Experimental conditions and parameters [10, 14, 30–33, 40, 42, 43, 46].

Experiment	Microscopic flow regime			Macroscopic self-leveling		
	Single-bubble injection	Multibubble injection	Bottom-heated boiling	Depressurization boiling	Bottom-heated boiling	Gas injection
Dimension	2D 3D	2D	2D	Large-scale 3D	Quasi-2d	Large-scale 3D
Viewing tank shape[a]	*R* *C*	*R*	*R*	*C*	*R*	*C*
Particle material	Glass, acrylic, Al_2O_3, ZrO_2	Glass	Glass	Al_2O_3, ZrO_2, SS, Pb	Glass, Al_2O_3, ZrO_2	Al_2O_3, ZrO_2, zn, SS, cu, Pb
Particle density (g/cm^3)	2.6~6.0	2.6	2.6	3.6~11.3	2.6~6.0	3.6~11.3
Particle size (mm)	0.4~6.0	0.4~6.0	0.4~6.0	0.5~6.0	0.4~6.0	0.3~6.0
Particle shape	Sphere	Sphere	Sphere	Sphere, non-sphere	Sphere	Sphere, non-sphere
Particle component	Single	Single	Single	Single	Single	Single, mixed
Water depth (mm)	250	400	400	250, 400	400	108~500
Heating intensity (W/cm^3)	—	—	Na[b]	0.08~0.43	—	—
Gas flow rate (L/min)	1.7×10^{-3}, 2.7×10^{-3}	1.0, 4.0	—	—	0~8.0	0~500
Bed height (mm)	30~200	250	200	100~160	180	90~200
Initial inclination angle (degree)	0	0	0	15~25	18~27	17~20

a: in this row, *R* and *C* represent "rectangular" and "cylinder", respectively. b: not available.

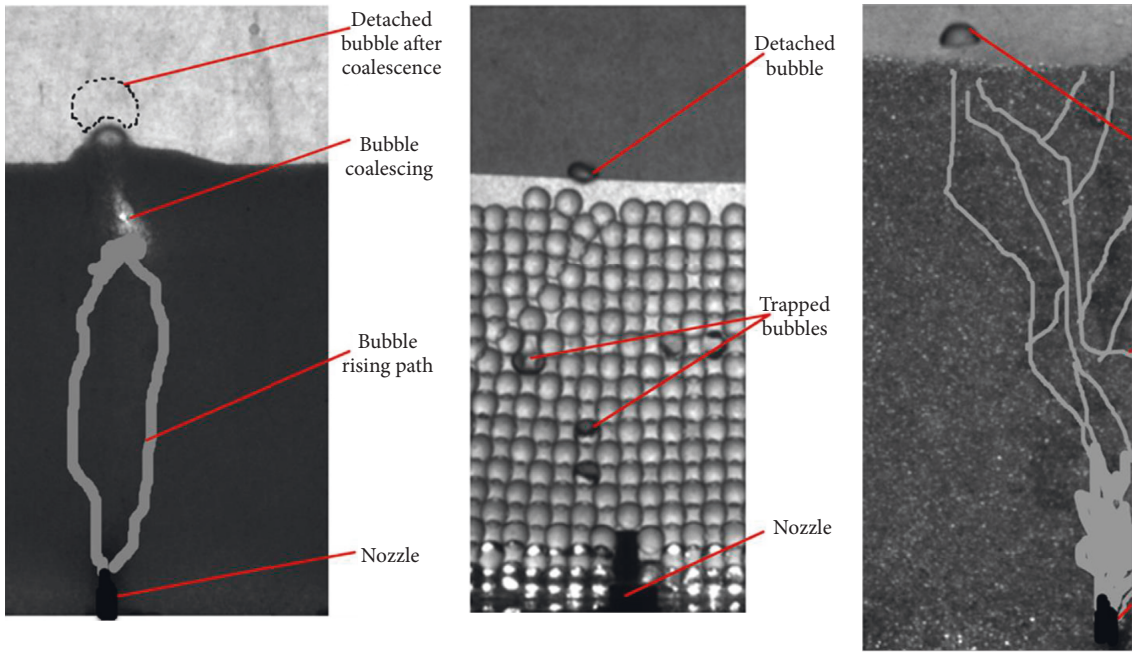

FIGURE 5: Typical bubble behaviors within particle beds [31] (a) Bubble coalescing regime (glass particles, dp = 0.4mm) (b) Bubble trapping regime (glass particles, dp = 6mm) (c) Transitional regime (glass particles, dp = 1mm).

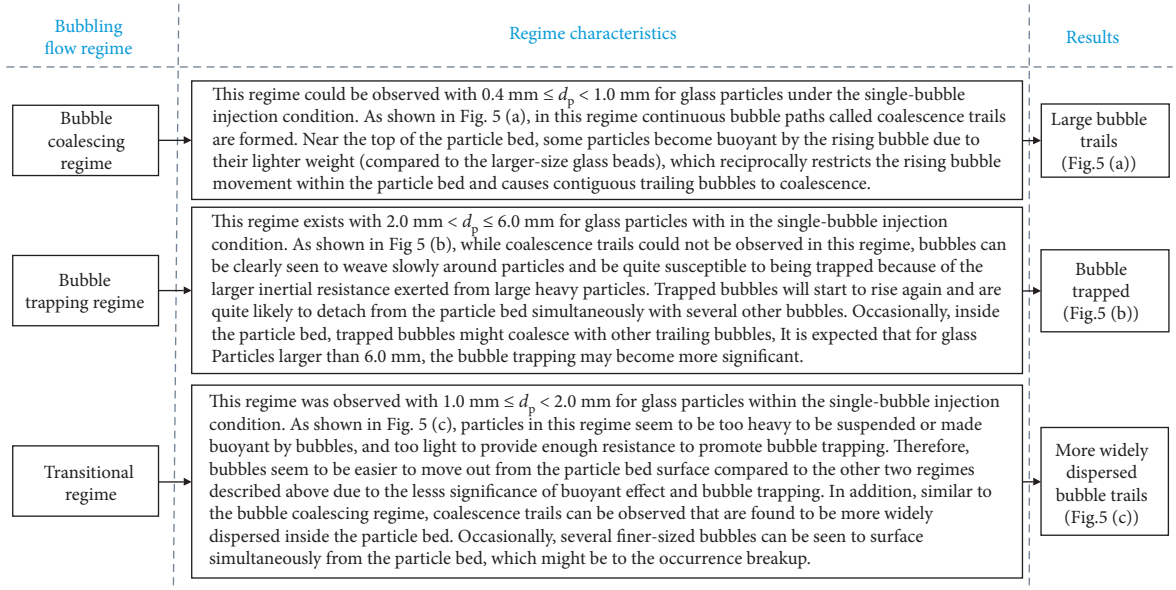

FIGURE 6: Flow regime characteristics of bubble behaviors within glass spherical particle beds in the experiments.

due to the enhancement of the bubble trapping, although the hydrophilicity of particle materials might be significant to affect the resistance (such as friction) exerted from the particles to the rising bubbles [31].

Furthermore, it has also been validated that the flow regime characteristics observed in the experiments with single-bubble injection could also support the experimental observations under multi-bubble injection and bottom-heated boiling conditions [32, 33]. Additionally, it was confirmed that aside from the properties of particle, the bubbling rate (i.e., injected gas flow rate or heating intensity) must also influence regime transitions [33]. Typically, the bubble coalescing regime was found to be easier to emerge since a larger bubbling rate had been employed. Therefore, it seems that all the performed investigations would suggest that the characteristics of the observed bubble behaviors (or flow regimes) should be common within wider ranges of conditions. The findings and understandings from microscopic flow regime experiments can provide significant arguments for studying and analyzing the macroscopic self-leveling mechanism and characteristics.

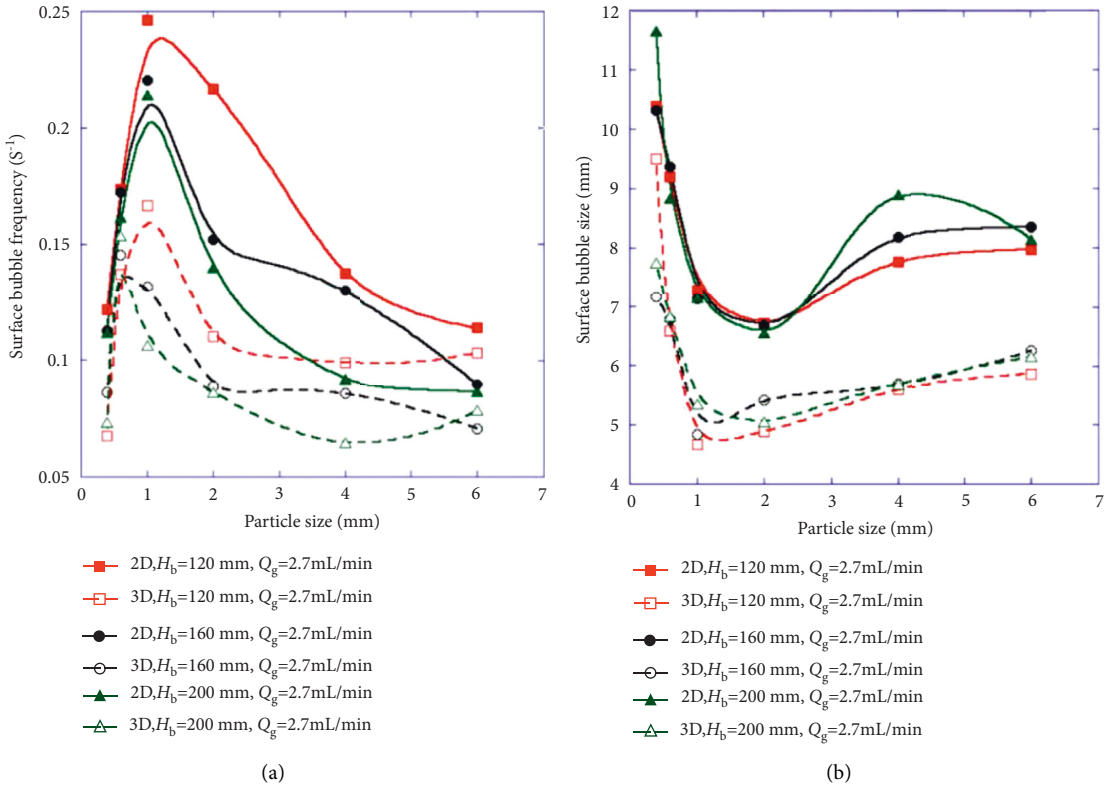

Figure 7: Effect of particle size on surface bubble frequency (glass particles) [31] (a) Surface bubble frequency (b) Surface bubble size.

2.2. Macroscopic Self-Leveling Behaviors

2.2.1. Experimental Conditions. As mentioned in Section 1, two kinds of boiling methods, namely depressurization boiling and gas-injection boiling, have been employed at the beginning of the macroscopic debris bed self-leveling investigations at Kyushu University and JAEA [10, 14] and IGCAR [30]. Figure 8 shows the experimental systems. For the depressurization cases, the vessel should be evacuated before starting experiments. In the experiment, the temperature inside the tank was kept at nearly 20 degrees to ensure the condensation of the generated steam flow. On the other hand, the bottom-heated boiling method was employed to supply a more persuasive argument verifying the reliability of the depressurization boiling method. In the experiments with bottom-heated boiling, the major apparatus was similar to that used in depressurization experiments, except the bottom region of the tank, which was equipped with a heater (see Figure 8(b)). Table 1 shows the detailed experimental conditions.

However, due to the difficulty of controlling and adjusting the gas phase, the nitrogen gas injection by adjusting gas pressure was employed to support predictive model development and further code validations [32]. After validating the effectiveness of the gas-injection method by comparing the experimental results with those using boiling methods under a similar effective gas flow rate [36], by employing various types of particles (including single-size spherical and non-spherical particles, mixed-size particles, mixed-density particles, and mixed-shape particles), extensive valuable results and knowledge were accumulated through gas-injection experiments at quasi-2D and 3D large-scale conditions. The experimental systems are shown in Figure 9. Detailed descriptions of experimental conditions are given in Table 1. Compared to the flow regime experiments, in the self-leveling ones, particles with larger densities were utilized to cover the probable debris proprieties in reactor accidents (e.g., densities from 7620 kg/m^3 for SS to 10,800 kg/m^3 for MOX fuel at 1000 K and sizes from 0.1 mm to several millimeters for fragmented debris [47]), and larger injected gas flow rates were utilized to trigger the onset of self-leveling behavior.

2.2.2. Experimental Results. To quantitatively estimate the transient leveling process, the inclination angle of the particle bed (see the definition shown in Figure 10) was investigated, and its variation was considered to represent the overall particle-bed shape variation. As a result, a normalized quantity $R(t)$ was defined (see equation (1)) to represent the bed shape variation so that the self-leveling behavior can be better qualified.

$$R(t) = \frac{\text{Inclination angle at time } t}{\text{Initial inclination angle (0 s)}}. \quad (1)$$

Figure 11 depicts the variations of $R(t)$ under different bubbling conditions. From Figure 11(a), it can be seen that

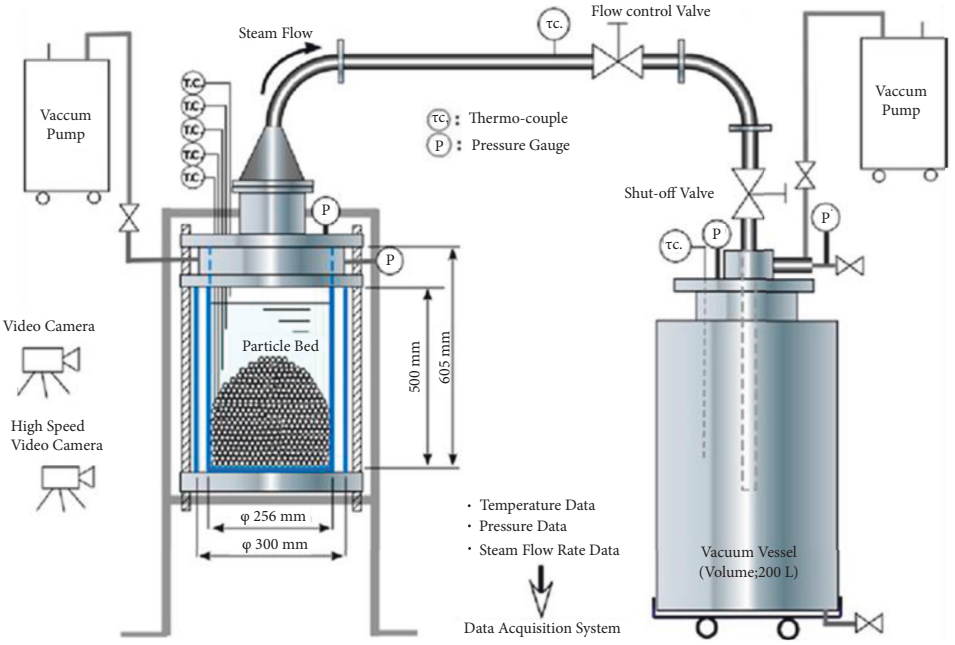

(a)

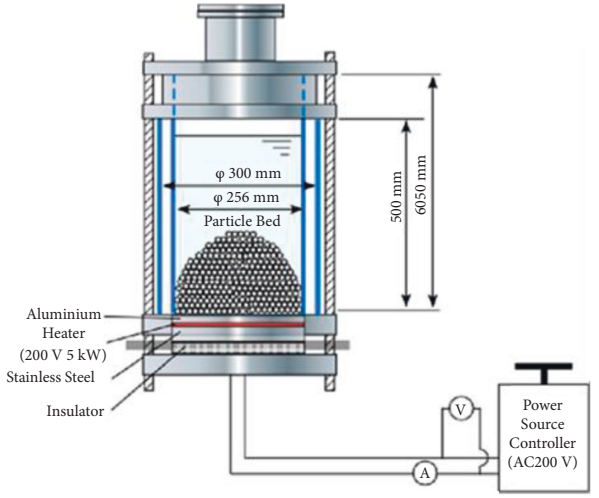

(b)

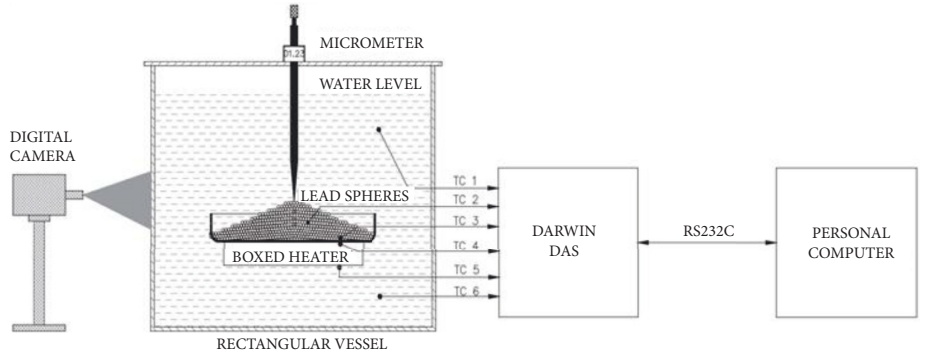

(c)

Figure 8: Self-leveling experimental systems with boiling methods [10, 30] (a) Depressurization boiling condition (b) Bottom-heated boiling condition (Kyushu University and JAEA) (c) Bottom-heated boiling condition (IGCAR).

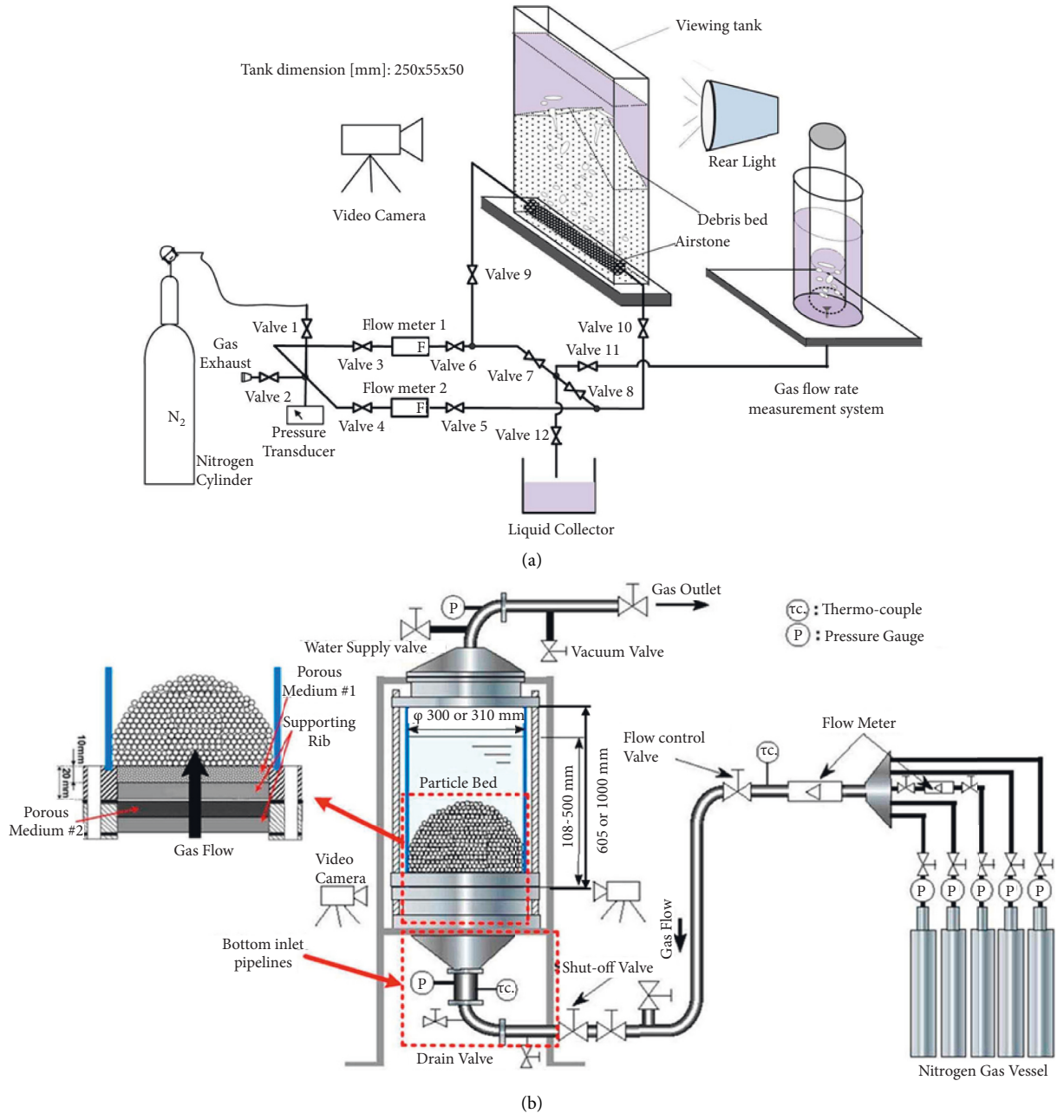

Figure 9: Schematic view of self-leveling experimental systems using gas-injection method [32, 36] (a) 2D system (b) 3D system.

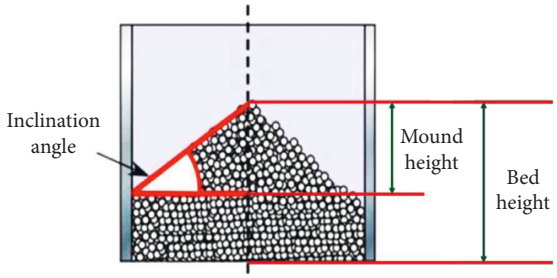

Figure 10: Schematic illustration for inclination angle, mound height and bed height.

similar self-leveling onset and development could be generally attained for different boiling cases (namely depressurization and bottom-heated) despite the existence of some observable microscopic differences (especially for the initial boiling area) [10]. It was also noted that for heavier particles (e.g., lead particles), the debris bed became more difficult to reach a perfect final horizontal level [30]. Comparing the bottom-heated and depressurization experiments, in general, a conclusion can be drawn is that the macroscopic self-leveling progression was not remarkably affected by the boiling modes. However, as shown in Figure 11(b), compared to the boiling method with a similar effective gas velocity U_g estimated in accordance with the energy

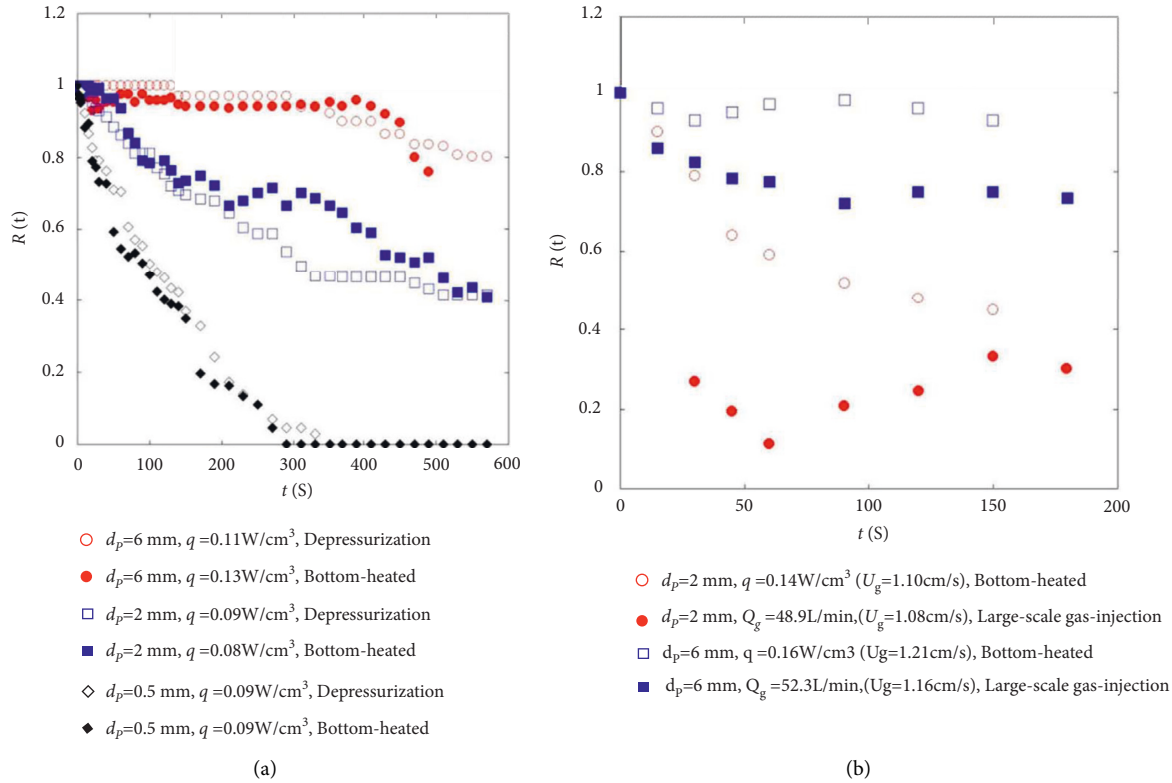

FIGURE 11: Effect of bubbling methods on R (t) (water depth = 400 mm, spherical alumina particles) [10, 32, 36] (a) Depressurization and bottom-heated methods (b) Gas-injection bottom-heated methods.

conservation by using the experimental power density q (see equation (2)), the self-leveling process proceeded faster when the gas-injection method was applied, which might mainly result from the different patterns of the "boiling" and "gas-percolation" in these two approaches. In the boiling experiments (i.e., bottom-heated and depressurization experiments), attention were focused on the early stage when subcooled boiling occurred [10], and thus, the steam was condensed and the boiling intensity was variable (for instance, the boiling intensity raised with the decrement of the water subcooling). However, in the experiments with the gas-injection method, to some extent, the simulated "boiling" possessed more characteristics of quasi-steady bulk boiling. Hence, for the gas-injection cases, a relatively larger gas flow intensity within the particle beds might result in observable faster progress of the self-leveling process, typically for particles with small sizes or densities during the initial stages.

$$U_g = \frac{V_b(1-\varepsilon)q}{A\left(C_p\Delta T_{\text{sub}}\rho_g + \rho_g h_v\right)} = \frac{H_b(1-\varepsilon)q}{C_p\Delta T_{\text{sub}}\rho_g + \rho_g h_v}. \quad (2)$$

Aside from the bubbling methods, other parameters would also significantly affect self-leveling development. As shown in Figure 12(a), according to the experimental observations regarding the evolution of R (t) [10, 36, 38, 40], it was found that the self-leveling process would proceed much slower in case of particles with larger inertia (i.e., larger-diameter or larger-density particles). Combining with the knowledge accumulated from the experimental studies on microscopic flow regime, it was expectable that this may due to the difficulty of the gas flow inside beds to move the particles with larger inertia. Moreover, if the particle beds were constituted by non-spherical particles, which possessed a smaller sphericity, the self-leveling development would be obviously restricted by the additional frictions and collisions between particles resulting from certain shape-related factors (such as roughness and eccentricity) [38]. Besides, a larger bubbling rate (namely boiling intensity or injected gas flow rate) can greatly enhance the self-leveling process (see Figure 12(b)), which may be explained in accordance with the flow regime observations: a more significant impetus for lifting solid particles became attainable with a larger bubbling rate, resulting in the bubble flow regime transitions (e.g., from bubble trapping regime to bubble coalescing regime), thereby promoting the self-leveling process. In addition, the injected gas could lead to the formation of more remarkable and violent liquid convections (particularly in case of higher water depth), as a result leading to faster variation of the inclination angle. These parametric trends were found in both 2D and 3D experiments. Nevertheless, based on the comparison between 2D and 3D cases with similar gas velocity U_g, it was

confirmable that the self-leveling process developed faster and more completely in 3D conditions, revealing that the wall effect is probably a prominent factor to play an astricting role in the bed shape variations [32, 36], although further investigations should be performed with the considerations of the differences in the mound-bed volumetric ratio in 2D and 3D conditions to clarify the effect of geometry differences on the self-leveling characteristics. Moreover, it was observed that the particle beds possessing a larger volume (i.e., particle bed with a higher part below the particle mound) seemed to accelerate the self-leveling process, which might be due to the change of the profile of gas velocity before gas flowed into the particle mound [43]. In addition, by utilizing different types of bottom gas-injection plate, it was confirmed that in the cases with the same injected gas flow rate, the non-homogeneous coolant boiling within the particle bed was also expected to affect the self-leveling process, especially in the cases where the gas flow was concentrated in the center region of the particle bed, leading the peak particles to transfer to the peripherical regions, thereby promoting the self-leveling development [40].

Regarding the effect of mixed particles, according to the experimental observations [42, 43], it was found that the self-leveling behavior would be significantly influenced by the components of the particle mixture. For instance, when particle mixtures were composed of mixed-density particles, the particle beds were observed to be more difficult to level off if there were more fractions of heavier particles (see Figure 13(a)). Therefore, it may be understood that if the average density of the mixture is larger, the self-leveling development will be slower, although an accurate comparison of the self-leveling process between mixed-density cases and cases with homogeneous particles might be necessary. Similarly, for mixed-size cases (see Figure 13(b)), the self-leveling process proceeded more slowly when larger particles constituted the particle beds (i.e., particle mixture with larger average particle size), indicating the restricting effect of the overall particle-bed inertia on the self-leveling development. Besides, according to the observations from experiments using mixed-shape particles (i.e., particle mixtures with spherical and non-spherical particles), it was demonstrated again that particles with small sphericities would dampen the self-leveling process due to the additional particle-particle interactions.

In summary, the microscopic flow regime experiments provided valuable knowledge on bubble-particle interactions, and three typical flow regimes, including bubble coalescing regime, transitional regime and bubble trapping regime, were captured. According to the useful flow regime arguments, through investigations on self-leveling behavior, it was understandable that because of the particle-particle and bubble-particle interactions inside the particle beds and the liquid pool, various parametric conditions (such as particle properties, bubbling rate, and liquid convection intensity) could significantly influence the self-leveling onset and progress. Knowledge and results attained from experimental observations are of great importance to promote the subsequent modeling investigations.

3. Modeling Investigations

Aiming at rationally predicting the debris bed self-leveling characteristics, according to the knowledge and understandings obtained from experimental investigations, the modeling investigations were also performed for predicting the self-leveling onset, inclination-angle variation, mound-height variation, and bed-height variation [14, 33, 35, 37–40, 42, 43, 46].

3.1. Modeling for the Self-Leveling Onset. To preliminarily predict the self-leveling onset, the topmost particle instead of the particle bed was focused [14]. It was assumed that the self-leveling phenomenon occurred if the topmost particle possessed a positive vertical velocity U_{top}, which is associated with the two-phase flow velocity U_{tp} and the relative velocity between the particle and the two-phase flow surrounding it U_{re}:

$$U_{top} = U_{tp} - U_{re}. \tag{3}$$

To determine U_{re}, the following assumptions were adopted: (1) the basic consideration of this model involved only single-sized spherical particles, and thus, for the cases with non-spherical particles, they should be replaced by the spherical particles with a same volumetric equivalent diameter in the prediction; (2) the net force applied was vanish (i.e., the particle was without acceleration); (3) for gas and liquid, no relative slippage exited around the particle; (4) the frictional forces with other particles were ignorable. Then, the U_{re} can be deduced in accordance with force balance [14]:

$$U_{re} = \left[\frac{4}{3}\left(\frac{\rho_p}{\rho_a} - 1\right)\frac{g d_p}{C_d}\right]^{1/2}, \tag{4}$$

where C_d stands for the dimensionless drag coefficient; ρ_a is the average fluid density for the two-phase flow around the particle, which is given by $\rho_a = \alpha\rho_g + (1-\alpha)\rho_l$, with α the dimensionless average void fraction for the cross-section at the average particle bed height. Empirically, α was calculated through:

$$\alpha = \alpha_{Exp} C_\alpha, \tag{5}$$

where C_α is the correction factor regulating the volume average void fraction α_{Exp} attained in accordance with experimental measurements and calculated by [14]

$$\alpha_{Exp} = \frac{\Delta V}{\varepsilon V_b}, \tag{6}$$

where ΔV means the measured volume increase of water (estimated from water-level elevation) after the bubbling.

As for the U_{tp}, by assuming that the mean flow area within the particle bed (a) can be determined by $a = A_{cr}\varepsilon^{2/3}$ with A_{cr} the cross-sectional area of the particle bed, it can be determined by combining equation:

$$U_{tp} = \frac{Q_g}{\alpha a} = \frac{A_{cr} U_g}{\alpha a}, \tag{7}$$

where Q_g signifies injected gas flow rate for gas-injection cases, or the equivalent vaporization rate for boiling cases.

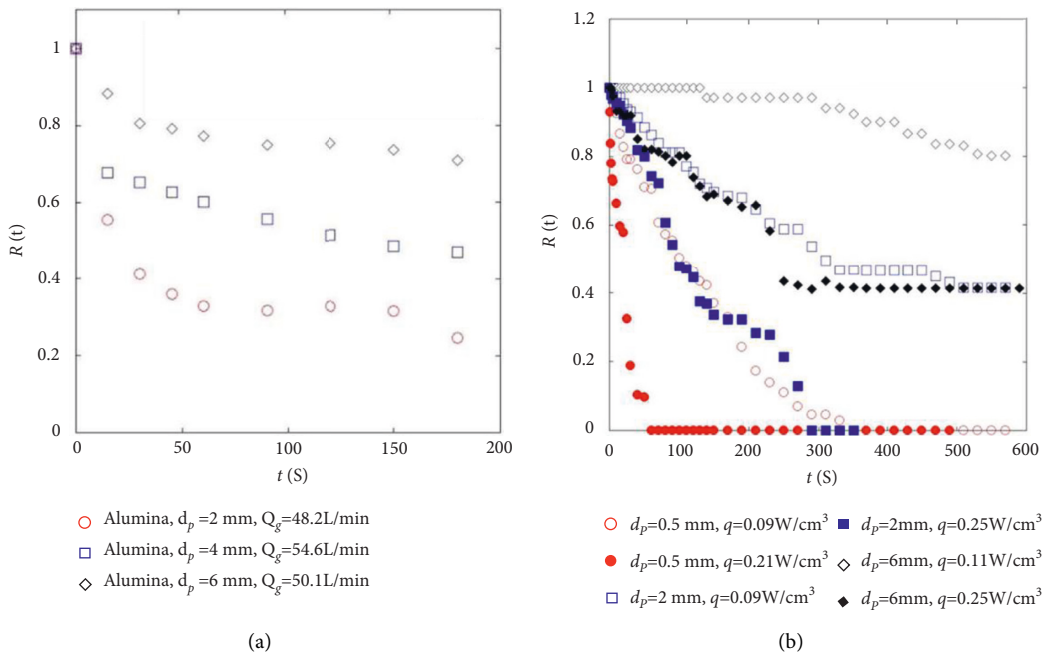

FIGURE 12: Effects of typical parameters on self-leveling development (spherical alumina particle) [10, 32, 36] (a) Effects of particle size (gas-injection condition) (b) Effects of bubbling rate (boiling condition).

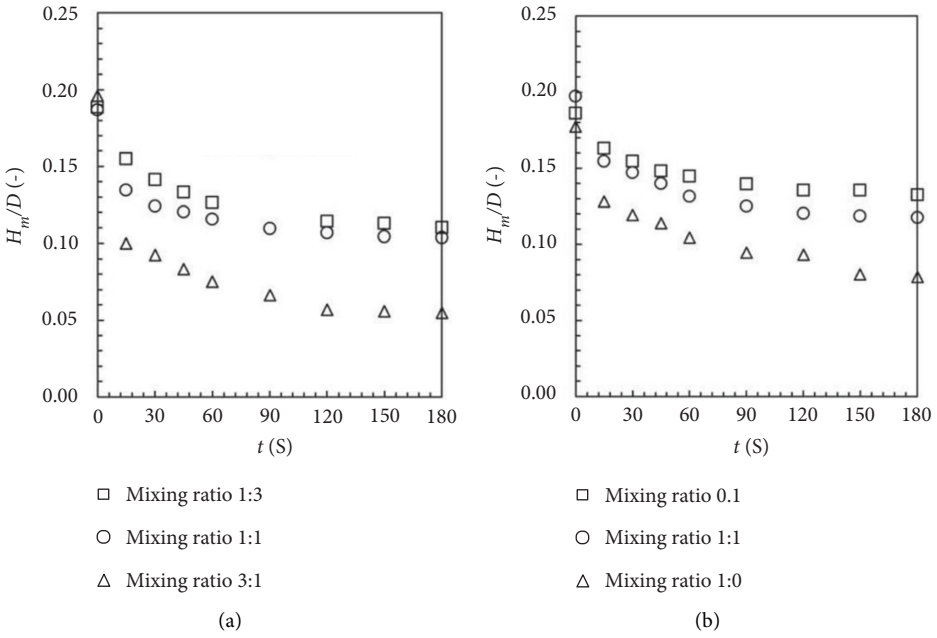

FIGURE 13: Self-leveling behavior for mixed particles with different volumetric mixing ratios [42, 43]. (a) Mixed density (Spherical Al2O3 and SS particles, dp = 2mm, Qg = 200L/min) (b) Mixed size (Spherical SS particles, dp = 2 and 4mm, Qg = 200L/min)

Typically, for boiling cases, by combining equation (2) and (7), U_{tp} becomes

$$U_{tp} = \frac{H_b(1-\varepsilon)q}{\alpha\varepsilon^{2/3}\rho_g\left(C_p\Delta T_{sub} + h_v\right)}. \quad (8)$$

According to the model validation on the basis of 31 experimental runs with boiling methods and 22 runs with gas-injection methods [14, 40], it was verified that this model could provide reliable prediction on the self-leveling onset. After the model validation, the experimental data could be expanded by extrapolating the model predictions to actual reactor conditions with some degree of confidence to attain more useful knowledge concerning the self-leveling behavior. Owing to analyses regarding the equilibrium particle bed height (i.e., the critical bed height that can ensure $U_{top} = 0$) for boiling conditions, the important effects of parameters could be overall verified under actual reactor conditions by

employing the predictive model. Noticing that lower equilibrium bed height (or in other words, a more completely leveled-off particle bed) indicates the easier onset of self-leveling behavior, as shown in Figure 14, smaller-size particles and higher power density can facilitate the self-leveling onset. This reveals that in an actual reactor accident, where typical debris sizes ranged from 0.1 to several millimeters and the normal decay heat levels were nearly 10 W/cm^3, the occurrence of self-leveling behavior may be easier to be found [14].

3.2. Modeling for Self-Leveling Inclination-Angle Variation. Though the onset model, in which many assumptions were used on the single topmost particle, could provide reliable predictions, it should be pointed out that the self-leveling onset may not be sufficient for estimating the integrated debris bed self-leveling progression. Focusing on this aspect, based on the experimental findings accumulated from depressurization and gas-injection studies by utilizing single-size solid particles, an empirical model for predicting the time variation of inclination angles was further developed [32, 34, 35, 37, 39]. The bottom-heated condition was not included for the reason that it had been confirmed from the experiments that the self-leveling progression for different boiling cases was generally in the similar manner despite some microscopic differences.

By referring to the modeling methods for determining the critical gas velocity for solid particle suspension [48–50], the following correlation was proposed to evaluate the inclination angle at a specific time t_0 chosen from experiments when the self-leveling process became slow at the later stage [32, 34, 35, 37, 39]:

$$R(t_0) = K_{\mathrm{NS},1}\left[K_1\left(\frac{U_g}{U_T}\right)^{a_1}\left(\frac{\mu U_T}{\sigma}\right)^{b_1}\left(\frac{\rho_p-\rho_l}{\rho_l}\right)^{c_1}\right], \quad (9)$$

where K_1, a_1, b_1, and c_1 are empirical constants; $K_{\mathrm{NS},1}$ is a correction factor for estimating the influence of nonspherical particles (to be discussed later); U_T represents the terminal velocity of solid particles estimating in accordance with Heywood tables (for large particles) and Stokes's law (for small particles) [51]. As for the dimensionless terms, U_g/U_T shows the effect of gas flow rate, and $\mu U_T/\sigma$ characterizes the interaction between fluid and solid particles, while the term $(\rho_p-\rho_l)/\rho_l$ represents the buoyancy impact.

To represent the transient self-leveling characteristics, the time changes of the $R(t)$ should be considered. For $R(t)$, theoretically speaking, the following conditions should be attained: (1) $R(t=0)=1$; (2) $R(t=t_0)=R(t_0)$; (3) $\forall t \geq 0$, $0 \leq R(t) \leq 1$. Therefore, to satisfy these conditions in the predictive model, the following dependence was assumed:

$$\frac{1-R(t)}{1-R(t_0)} = \left(\frac{t}{t_0}\right)^n, \quad (10)$$

where n (with $0 \leq n \leq 1$) is a characteristic number representing the average variation rate of the inclination angle. For example, the slower the leveling progression, the larger the n. At the extreme, if the self-leveling rate is adequately slow, n tends to be 1. Noticing that the self-leveling rate should be different under different experimental conditions, n should be capable to be determined from the experimental parameters affecting the self-leveling development. Similarly, to determine the value of n by the experimental parameters, the second correlation was proposed:

$$n = K_{\mathrm{NS},2}\left[K_2\left(\frac{U_g}{U_T}\right)^{a_2}\left(\frac{\mu U_T}{\sigma}\right)^{b_2}\left(\frac{\rho_p-\rho_l}{\rho_l}\right)^{c_2}\right], \quad (11)$$

where K_2, a_2, b_2 and c_2 are empirical constants; $K_{\mathrm{NS},2}$ is a correction factor for estimating the influence of particle-shape parameters.

Owing to linear regression analysis for the logarithmic forms of equations (9) and (11) [34, 35, 37], the empirical constants were empirically obtained under different conditions (see Table 2). While for $K_{\mathrm{NS},1}$ and $K_{\mathrm{NS},2}$, the following functional form was suggested to ensure the consistency for spherical particles (i.e., $K_{\mathrm{NS},1}$ and $K_{\mathrm{NS},2}$ should be equal to 1.0 in cases of spherical particles):

$$K_{\mathrm{NS},i} = 1.0 + s_{i,1}\frac{(1-\phi)^{s_{i,2}}}{\left(\mathrm{Re}_g\right)^{s_{i,3}}}, \quad (12)$$

where Re_g is the gas Reynolds number; $s_{i,1}$, $s_{i,2}$ and $s_{i,3}$ are empirical constants listed in Table 2; ϕ means the sphericity of solid particles, which was calculated by using Ergun's equation in accordance with the measured pressure drop (ΔP):

$$\frac{\Delta P}{H_b} = 150\frac{(1-\varepsilon)^2}{\varepsilon^3}\frac{\mu_f}{(\phi d_{\mathrm{ev}})^2}U_f + 1.75\frac{(1-\varepsilon)}{\varepsilon^3}\frac{\rho_f}{\phi d_{\mathrm{ev}}}U_f^2. \quad (13)$$

Figure 15 shows the comparison of $R(t)$ between experiments and model predictions. Generally, it is observable that regardless of the bubbling condition (gas injection or depressurization boiling), the particle shape (sphere or nonsphere) and the dimension experimental systems (2D or 3D), the capability and reliability of this model in predicting the variation of inclination angles could be confirmed.

Motivated to improve the validity and reliability of the model, the crucial parametric effects were also studied by comparing the experimental observed and modeling predicted variation of $R(t)$ [34, 35, 37]. For instance, Figure 16 shows the good agreement between the model predictions and experimental observations on the effect of particle size. However, it should be recognized that with different bubbling methods, the values of corresponding empirical constants (see Table 2) were not similar. This might be caused by not only the differences in experimental systems (e.g., dimensions and bubbling methods), but also the differences in selecting the specific time t_0 (i.e., 300 s, 180 s, and 100 s for 2D gas injection, 3D gas injection and 3D depressurization, respectively). It can be easily understood that the values of $R(t_0)$ should be different when different t_0 was selected, causing different values of empirical constants in equations (9) and (11). Therefore, to attain a more generalized model that can be utilized under different conditions (including actual reactor accidental conditions), it is still required to perform more experimental investigations to elucidate these differences.

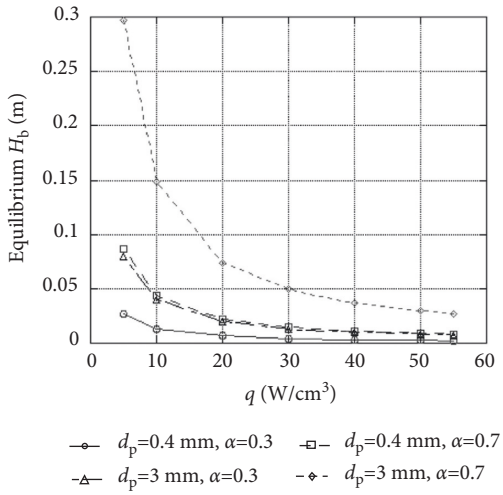

FIGURE 14: Extrapolation analyses to actual reactor conditions by the onset model [14].

3.3. Modeling for Self-Leveling Mound- and Bed-Height Variation. Considering that the particle mound and bed heights were also the key influencing factors for the ability of cooling of debris beds, aimed at obtaining more valuable predictions for evaluating the debris bed self-leveling behavior, another model, which is applicable to predict the mound-height variation, was established in accordance with the 3D gas-injection experiments using single-size particles with shapes of the sphere and non-sphere [46]. While further noticing from the experiments that the heights of the lower part of particle beds (i.e., the volume of particle bed) could also play a significant role in the self-leveling development, a model for estimating the transient bed height was also developed on the basis of the gas-injection experiments for single and mixed particles [43].

The model for describing the time variation of the mound height $H_m(t)$ was developed as [46]

$$\frac{H_m(t) - H_{m,\text{level}}}{H_m(t = 0\,\text{s}) - H_{m,\text{level}}} = \left(1 + \frac{t}{\tau}\right)^{-1}, \tag{14}$$

where $H_{\text{m,level}}$ is the completely leveled-off mound height (i.e., the height of mound at $t = \infty$), and τ stands for the characteristic time constant, which was dependent on the rate of self-leveling progression. Suggesting that the fluid and particle properties and the gas velocity should noticeably influence the values of $H_{m,\text{level}}$ and τ, the following correlations were determined for $H_{m,\text{level}}$ and τ [46]:

$$\frac{H_{m,\text{level}}}{D} = K_1'\left(\frac{U_g}{U_T}\right)^{a_1'}\left(\frac{A_p}{D^2}\right)^{b_1'}\left(\frac{d_p}{D}\right)^{c_1'}\varepsilon^{d_1'}\text{Re}_g^{e_1'}\text{Ar}_g^{f_1'}, \tag{15}$$

and

$$\%\,\frac{\tau U_g}{D} = K_2'\left(\frac{U_g}{U_T}\right)^{a_2'}\left(\frac{A_p}{D^2}\right)^{b_2'}\left(\frac{d_p}{D}\right)^{c_2'}\varepsilon^{d_2'}\text{Re}_g^{e_2'}\text{Ar}_g^{f_2'}, \tag{16}$$

where K_i' and $a_i' \sim f_i'$ (i = 1 and 2) are empirical constants; A_p is the actual particle surface area, and the term A_p/D^2 characterizes the restricting effect on self-leveling development resulted from larger surface area or interparticle frictions [46]; Ar_g is the gas-phase Archimedes number = $(\rho_g(\rho_p - \rho_l)gd_p^3/\mu_g^2)$ for buoyed solids.

Similarly, for the modeling of time variation of bed height $H_b(t)$, the empirical model becomes [43]

$$\frac{H_b(t) - H_{b,\text{level}}}{H_b(t = 0\,\text{s}) - H_{b,\text{level}}} = \left(1 + \frac{t}{\tau}\right)^{-1}, \tag{17}$$

and the following correlations were adopted:

$$\frac{H_{b,\text{level}}}{D} = K_3'\left(\frac{U_g'}{U_T}\right)^{a_3'}\left(\frac{A_p}{D^2}\right)^{b_3'}\left(\frac{d_p}{D}\right)^{c_3'}\left(\frac{V_b(1-\varepsilon)}{d_p^3}\right)^{d_3'}\text{Re}_g^{e_3'}\text{Ar}_g^{f_3'}, \tag{18}$$

and

$$\frac{U_{\text{level}}}{U_g'} = K_4'\left(\frac{U_g'}{U_T}\right)^{a_4'}\left(\frac{A_p}{D^2}\right)^{b_4'}\left(\frac{d_p}{D}\right)^{c_4'}\left(\frac{V_b(1-\varepsilon)}{d_p^3}\right)^{d_4'}\text{Re}_g^{e_4'}\text{Ar}_g^{f_4'}, \tag{19}$$

where K_i' and $a_i' \sim f_i'$ (i = 3 and 4) are the empirical constants; $U_{\text{level}} = H_b(t = 0\,\text{s}) - H_{b,\text{level}}/\tau$ represents the characteristic leveling velocity regarding the particle bed heights; $U_g' = U_g/\varepsilon$ is the actual gas velocity corrected from U_g with the consideration of the influence of porosity on the gas movements [43]; $V_b(1-\varepsilon)/d_p^3$ is introduced instead of ε to evaluate the effect of particle volume (i.e., the height of the lower part of particle bed).

To attain more evident comparisons between different experimental cases, the initial mound and heights in the models were adjusted to the same values. As a result, the time constant τ should be corrected to τ' as follows:

$$\tau' = \tau\left(1 + \frac{t^*}{\tau}\right), \tag{20}$$

with

$$t^* = \tau\frac{H_m(t = 0\,\text{s}) - H_{m0}}{H_{m0} - H_{b,\text{level}}}\ \text{or}\ \tau\frac{H_b(t = 0\,\text{s}) - H_{b0}}{H_{b0} - H_{b,\text{level}}}, \tag{21}$$

where H_{m0} (or H_{b0}) is the chosen mound (or bed) height being the initial mound (or bed) height for the modeling investigations; t^* is the time when the H_{m0} (or H_{b0}) was achieved in the experiments.

Furthermore, to improve the reliability of the model prediction under mixed-particle conditions, it is expectable that for the particle mixture, its overall hydraulic performance can be characterized by some equivalent quantities [52–54]. In this modeling study, the particle diameter d_p for the particle mixture was attained by its volumetric equivalent diameter d_{ev}:

$$d_{\text{ev}} = \left[\frac{\sum_{i=1}^{N}\left[V_{pi}(1-\varepsilon_i)\right]}{\sum_{i=1}^{N}\left[V_{pi}(1-\varepsilon_i)/d_{pi}^3\right]}\right]^{1/3}, \tag{22}$$

Table 2: Empirical constants determined for the model of $R(t)$ [33, 34, 35].

Empirical constant	Gas injection (2D)	Gas injection (3D)	Depressurization (3D)
$\ln(K_1)$	2.154	0.671	−0.690
a_1	−0.371	−0.100	−0.432
b_1	1.553	0.635	−0.0195
c_1	0.504	0.465	−0.183
$\ln(K_2)$	−1.101	0.550	−0.337
a_2	−0.355	−0.105	−0.287
b_2	0.100	0.745	0.0504
c_2	0.100	0.445	−0.144
$s_{1,1}$	—	3.419	—
$s_{1,2}$	—	1.171	—
$s_{1,3}$	—	0.527	—
$s_{2,1}$	—	8.062	—
$s_{2,2}$	—	1.317	—
$s_{2,3}$	—	0.572	—

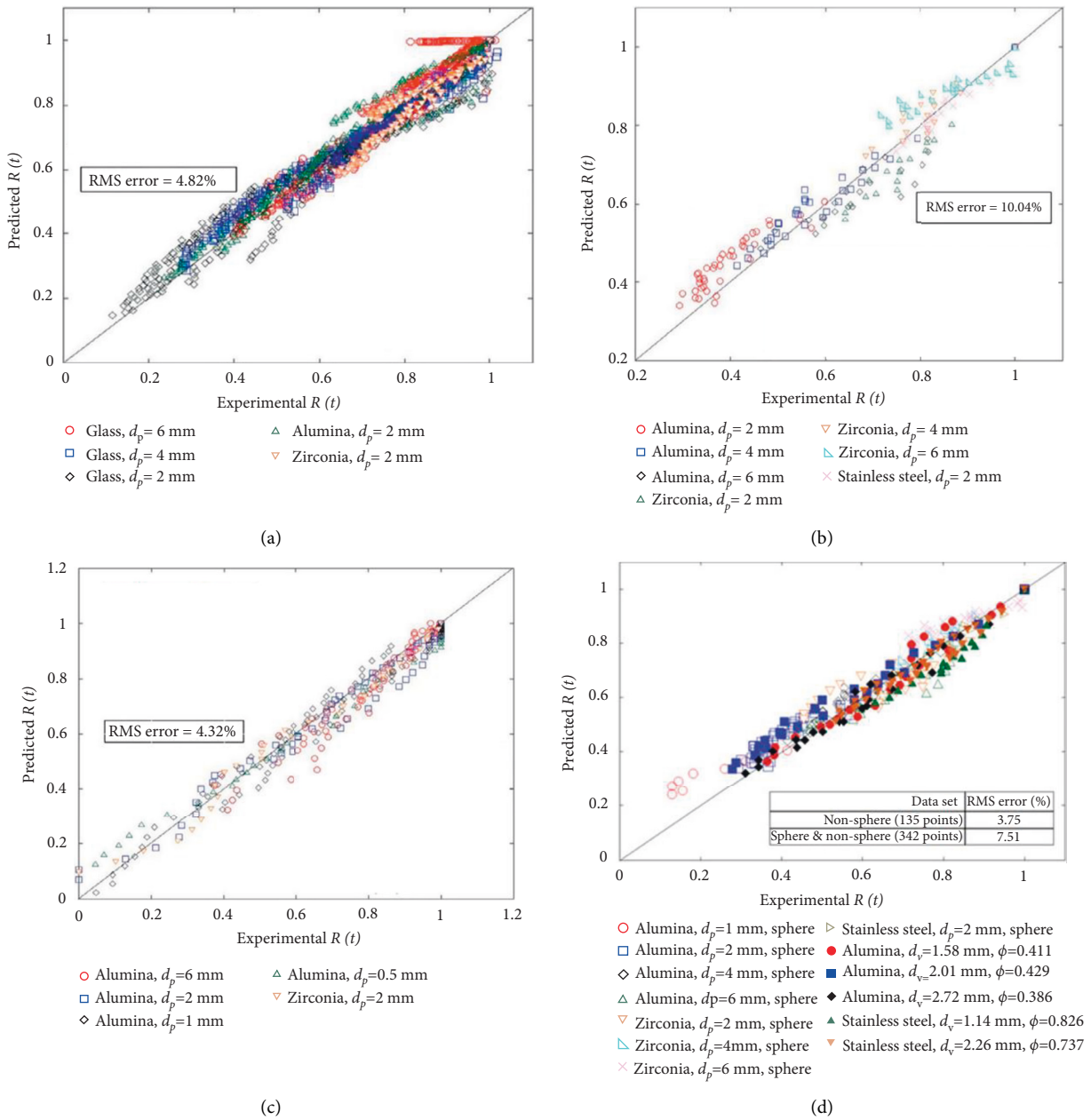

Figure 15: Comparison of experimental and predicted $R(t)$ for different experimental conditions [37, 38] (a) 2D gas injection, spherical particles (b) 3D gas injection, spherical particles (c) 3D Depressurization, spherical particles (d) 3D gas injection, spherical and non-spherical particles.

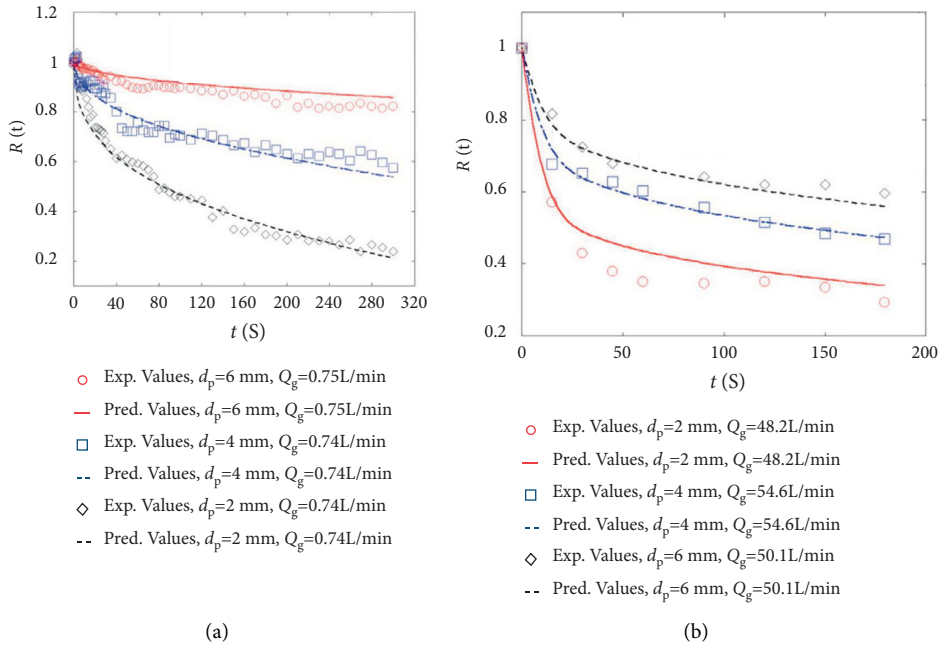

FIGURE 16: Comparisons of experimental and predicted results for the effect of particle size on *R (t)* [37] (a) 2D gas-injection condition (b) 3D gas-injection condition.

TABLE 3: Empirical constants determined for the models of mound and bed heights [43, 46].

Empirical constant	$i = 1$	$i = 2$	$i = 3$	$i = 4$
$\ln(K_i')$	−39.212	−24.583	−4.12	8.29
a_i'	0.75207	−2.5196	−0.377	9.37
b_i'	−0.11316	4.2759	1.24	−22.0
c_i'	−2.6374	−11.266	−0.383	28.7
d_i'	−1.3640	−0.30864	−0.0216	4.04
e_i'	−1.0555	3.1129	0.836	−5.89
f_i'	1.7079	−0.44302	0.345	−10.1

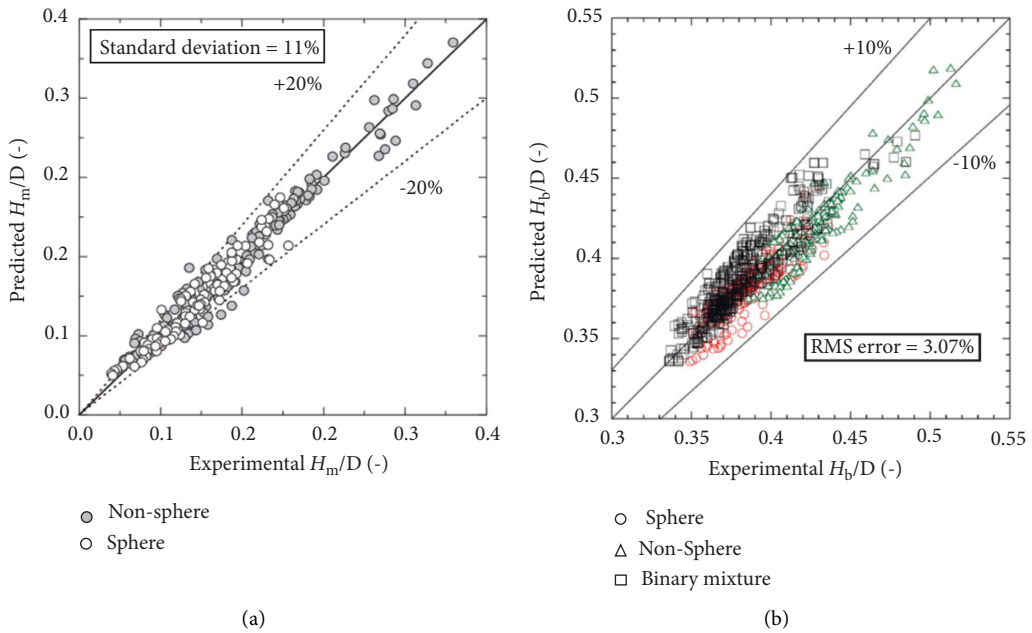

FIGURE 17: Comparison of mound and bed heights between experiments and modeling predictions [43, 46] (a) Mound height (b) Bed height.

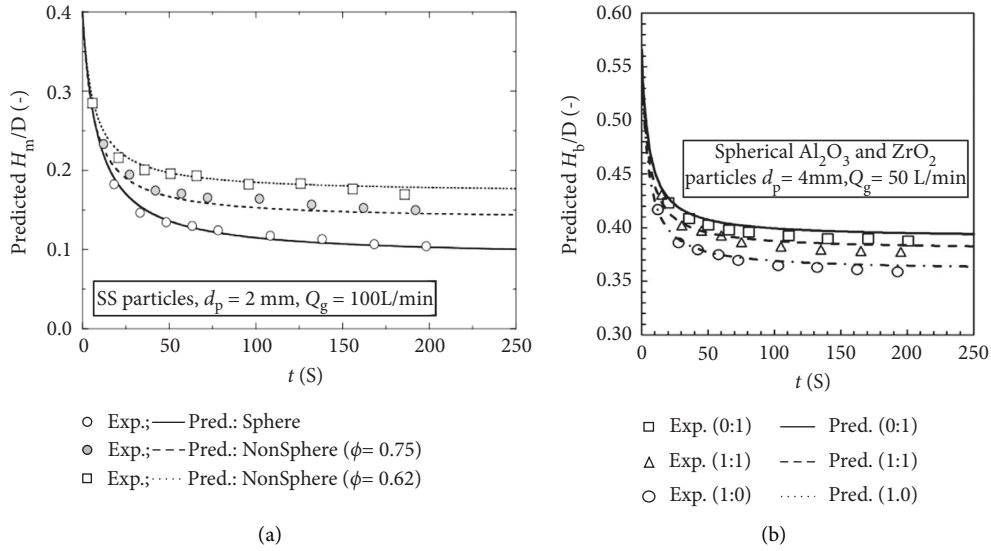

Figure 18: Variations of mound and bed heights in experiments and modeling predictions [43, 46] (a) Effect of particle shape on variation of *Hm* (b) Effect of mixed-density on variation of *Hb*.

and the particle density ρ_p could be determined by its mass equivalent density ρ_{ev}:

$$\rho_{ev} = \frac{\sum_{i=1}^{N} V_i(1-\varepsilon_i)\rho_{p_i}}{\sum_{i=1}^{N} V_i(1-\varepsilon_i)}, \quad (23)$$

where the subscript i stands for the i-th component of the particle mixture; while N is the total number of particle components.

Based on the regression analysis for equations (15), (16), (18), and (19) in accordance with experimental data [43, 46], the empirical constants were determined (see Table 3). As displayed in Figure 17, the accuracy for the prediction results of these two models was verified, and the model reliability was confirmed. To further validate the reliability of these models, as displayed in Figure 18, the effects of various parameters were also verified by comparing the experimental observations and modeling predictions on the variations of mound and bed heights.

In a short, to effectively predict the self-leveling behavior, based on a huge number of experimental data accumulated with the consideration of various key parameters, the empirical models for predicting the self-leveling onset, the inclination-angle variation, and the mound, as well as bed-height variations, were developed separately. Despite the different focusing points, every model can provide reasonable and reliable predictions for the corresponding self-leveling characteristics under specific conditions. However, it should be noted that the onset model, which was the first model developed for assessing the self-leveling behavior, could not sufficiently predict the transient behavior during the self-leveling process, and the assumptions for the model establishment are still required to be carefully evaluated. On the other hand, more detailed self-leveling configurations could be predicted from the models for inclination-angle variation and mound-as well as bed-height variations. The applicable conditions for the inclination-angle model and the mound- or bed-height model may be different up to the different core-catcher designs for SFRs (e.g., single-layer core catcher for CFR 600, multi-layer core catcher for JSFR) [55], which will be explained later in Section 4. Further, it should also be pointed out that because of the limitations that existed in the experiments performed by using the simulant materials, some validated ranges of parameters (such as heating power) taken into account in the modeling development might be insufficient. Nevertheless, knowledge attained from predictive modeling developments and extended analyses (e.g., extrapolation) should provide certain evidence along with confidence in further computer model developments and verifications [45].

4. Conclusion

Since the debris bed's self-leveling behavior can be an important triggering factor for the transfer of fuel debris and can notably influence the heat-removal capability of the debris bed, which is of significance to the evaluation of the accident progress, the experimental and modeling investigations on this behavior are greatly important to the improvement of structural designs of the relevant safety devices in SFR (e.g., the core catcher) for ensuring the IVR. In the past decade, considering the initially convex (or conical) shape of debris beds, lots of valuable knowledge were accumulated through the relevant experimental and modeling investigations.

For the experimental investigations, to obtain important knowledge to support the understanding of the debris bed self-leveling behavior, based on the direct visualization evidence captured in the observations from the microscopic flow regime experiments, the mechanism and characteristics of bubble behaviors inside the particle beds (esp. bubble-particle interaction) were investigated. According to the experimental analysis, the noticeable effects of various parameters (such as the effect of particle properties, effect of

gas-related parameters, and wall effect) on the flow regime transitions were identified, providing a more comprehensive understanding of the self-leveling behaviors. While in the macroscopic self-leveling experimental investigations, three bubbling methods for simulating the coolant (i.e., sodium) boiling, including depressurization, bottom heating, and gas injection, were applied for studying the self-leveling characteristics and relevant parametric effects on self-leveling development. Though similar tendencies of self-leveling development could be found under different bubbling conditions, it should still be noticed that as compared to the boiling cases (i.e., depressurization and bottom-heated boiling), more rapid self-leveling progression was found for the gas-injection cases, which was used to simulate the quasi-steady bulk boiling condition rather than the early subcooled boiling condition.

Regarding the modeling investigations, based on the experiments utilizing depressurization and gas injection, the applicability and reliability of the predictive model established for the self-leveling onset were validated. According to the extrapolated analyses by employing the onset model, it was expected that such a self-leveling phenomenon is probable to become easier to occur under actual reactor accident conditions. However, it should be recognized that in this model focusing on the movement of the topmost particles, lots of influences and interactions within the particle beds were not taken into account, and therefore, its applicability for predicting the transient self-leveling behaviors was restricted. In addition, the assumptions for this model establishment should also be carefully evaluated although good agreements between experiments and predictions could be attained in the current stage. Focusing on these points, the predictive models focusing on the time variation of inclination angle $R(t)$, mound height $H_m(t)$, and bed height $H_b(t)$ were established for the more comprehensive evaluations of the debris bed self-leveling behavior. It was found that the transient behaviors, as well as the parametric effects, could be reasonably and reliably reproduced by employing these models. However, considering the different designs of core catcher for SFRs (e.g., single-layer core catcher for CFR 600, multi-layer core catcher for JSFR) [15, 55], we suggest that the applicable situations for these models may be different. For an SFR with a single-layer core catcher, in the CDAs, initially, the debris bed is mostly formed with a larger inclination angle due to the lack of the interlayer transfer of debris. Therefore, regarding the model development, the predictive model for $R(t)$ that is considered more for the early fast leveling periods, in which the self-leveling behavior plays a more prominent role in the debris bed ability of cooling, may be more appropriate to apply in such cases. On the other hand, in the models of $H_m(t)$ and $H_b(t)$, which are established in accordance with the completely leveled mound and bed heights (i.e., the mound and bed heights at $t=\infty$), the early fast leveling stage may not be comparatively precisely estimated, even applying the extrapolation method. However, noticing the fact that for SFRs designed with a multi-layer core catcher, the moderate inclination angles are probably to be initially attained due to the possibility of interlayer transfer of debris, these models for predicting the mound and bed heights seem to be more suitable and applicable for analyzing the self-leveling behavior in such cases, especially with the consideration of the requirement of long-term evaluation for the heat-removal capacity of debris bed. In conclusion, owing to these predictive models, despite their different focal points, the debris bed self-leveling onset and its transient behaviors can be well predicted under specific conditions, thereby providing confidence for the development of more reliable and more generalized predictive models to realize their applicability for more realistic cases. Knowledge from the experimental and modeling investigations is supposed to be valuable for improving the designs for an in-vessel core catcher (s) of SFR and enhancing the developments and validations of relevant computer models (such as models for evaluating bubble-solid and solid-liquid interaction) involved in SFR safety analysis codes.

5. Future Prospects

Though lots of insights into the characteristics and mechanism of the self-leveling behavior were gained from the experimental and modeling investigations over the past decade, it is necessary to point out that for evaluating an actual CDA of SFR, the situations considered in the past studies are still insufficient. Therefore, to attain more useful knowledge for the SFR severe accident analyses regarding the self-leveling behavior, it is still required to perform further experimental and modeling investigations, which may be included but are not limited to the following possibilities:

(1) Further experimental investigations and modeling verifications (or developments) in the case of other initial bed shapes. According to the recent visualization experimental and modeling research on debris bed formation behavior [8, 12, 56–58], it was clarified that under different parametric conditions with considerations of a typical CDA of SFR, not only the convex bed, but also the flat, concave and trapezoid beds would possibly form due to the different interparticle and particle-fluid interactions. However, in the past self-leveling investigations, it was assumed that the particle bed was initially convex, which was inadequate to take all possible initial debris bed shapes into account. It is reasonably expectable that the self-leveling process and characteristics should be quite different from other initial bed shapes. Therefore, focusing on this aspect, further experiments can be conducted by employing different initial particle bed shapes (such as concave and trapezoid shapes) to more comprehensively clarify the debris bed self-leveling behavior. Subsequently, the predictive models established may be verified or further developed in accordance with the experimental observations and data obtained.

(2) Further investigations for effects of mixed particles with the consideration of particle separation and

stratification. From the recent studies focusing on the debris bed formation behavior by utilizing mixed particles (including mixed-size and mixed-density particles) [13, 59], it was pointed out that during the debris sedimentation and accumulation process, different particle components are probable to have different behaviors because of the difference in their particle inertia, indicating the latent particle stratification and separation in some typical accident situations (e.g., sodium boiling violently). However, in the past investigations on the debris bed self-leveling behavior by using mixed particles [42, 43], the particle beds were composed of fully uniformly mixed particles. Combining the understandings attained from these studies, it is rationally imaginable that the debris bed self-leveling behavior would also be influenced by the effects of such separation and stratification. Therefore, further experimental investigations along with modeling developments can be prepared with the consideration of particle separation and stratification existing in the particle bed.

(3) Coupling investigations on debris bed formation and self-leveling behaviors. Based on the experimental studies on the debris bed formation behavior with bubble generations (including bottom heating and gas-injection) for the simulation of the sodium boiling condition induced by the decay heat generated from accumulated debris beds [60, 61], it was observed that the self-leveling behavior could be found simultaneously with the debris bed sedimentation and accumulation process. Hence, it can be reasonable to suggest that these two debris bed behaviors might emerge together in an actual accident. Therefore, investigations for elaborating on the synchronous influence of sodium boiling on the two phenomena and the impact of falling particles on the self-leveling process might be also of some interest.

Nomenclature

Symbols

a: Mean flow area in debris bed (mm^2)
A: Area (mm^2)
Ar: Archimedes number (–)
C_d: Drag coefficient (–)
C_p: Specific heat capacity (J/(kg·K))
d: Diameter (mm)
D: Inner diameter of experimental device (mm)
g: Gravitational acceleration (m/s^2)
H: Height (mm)
h_v: Heat of vaporization (J/kg)
m: Mass (kg)
q: Heating power (W/cm^3)
Q: Flow rate (L/min)
$R\ (t)$: Variation of inclination angle (degree)
Re: Relative quantity
t: Time (s)
t_0: Specific time selected (s)
U: Velocity (m/s)
V: Volume (L)
ΔP: Pressure drop (Pa)
ΔT_{sub}: Subcooled degree (K)
ΔV: Volume increase of water after the bubbling (L)

Greek letters

α: Average void fraction (–)
μ: Viscosity (Pa·s)
σ: Surface tension (N/m)
τ: Characteristic time constant (s)
ϕ: Particle sphericity (–)
ε: Bed voidage (–)
ρ: Density (kg/m^3)

Subscripts

a: Average
b: Particle bed
cr: Cross section
ev: Equivalent
Exp: Experiment
f: Fluid
g: Gas
l: Liquid
level: Level-off
m: Particle mound
p: Particle
re: Reynolds number (–)
T: Terminal
top: Topmost particle
tp: Two-phase fluid.

Conflicts of Interest

The authors declare that there are no conflicts of interest regarding the publication of this article.

Acknowledgments

This work was financially supported by Guangdong Provincial Science and Technology Plan Project (no. 2021A050 5030026) and the Basic and Applied Basic Research Foundation of Guangdong Province (no. 2022A1515011582) in China.

References

[1] B. Raj, P. Chellapandi, and P. V. Rao, *Sodium Fast Reactors with Closed Fuel Cycle*, CRC Press, Boca Raton, FL, USA, 2015.
[2] H. Ohshima and S. Kubo, *Handbook of Generation IV Nuclear Reactors*, Woodhead Publishing, Manchester, England, 2016.
[3] N. Kasahara, *Fast Reactor System Design*, Springer Nature Singapore, Tokyo, Japan, 2017.
[4] Oecd Nuclear Energy Agency, *Technology Roadmap Update for Generation IV Nuclear Energy Systems*, Generation IV International Forum (GIF), Paris, France, 2014.
[5] R. Xu and S. Cheng, "Review of the molten-pool sloshing motion in case of core disruptive accident: experimental and modeling studies," *Progress in Nuclear Energy*, vol. 133, Article ID 103647, 2021.
[6] J. F. Marchaterre, "Overview of core disruptive accidents," *Nuclear Engineering and Design*, vol. 42, no. 1, pp. 11–17, 1977.

[7] W. Maschek, R. Li, C. Matzerath Boccaccini, F. Gabrielli, and K. Morita, "Investigation on upper bounds of recriticality energetics of hypothetical core disruptive accidents in sodium cooled fast reactors," *Nuclear Engineering and Design*, vol. 326, pp. 392–402, 2018.

[8] S. Lin, S. Cheng, G. Jiang et al., "A two-dimensional experimental investigation on debris bed formation behavior," *Progress in Nuclear Energy*, vol. 96, pp. 118–132, 2017.

[9] S. Cheng, S. Wang, G. Jiang et al., "Development and analysis of a regime map for predicting debris bed formation behavior," *Annals of Nuclear Energy*, vol. 109, pp. 658–666, 2017.

[10] B. Zhang, T. Harada, D. Hirahara et al., "Experimental investigation on self-leveling behavior in debris beds," *Nuclear Engineering and Design*, vol. 241, no. 1, pp. 366–377, 2011.

[11] A. Tentner, E. Parma, T. Wei, and R. Wigeland, *Severe Accident Approach-Final Report. Evaluation of Design Measures for Severe Accident Prevention and Consequence Mitigation*, Argonne National Laboratory, Lemont, IL, USA, 2010.

[12] M. Shamsuzzaman, T. Horie, F. Fuke et al., "Experimental study on debris bed characteristics for the sedimentation behavior of solid particles used as simulant debris," *Annals of Nuclear Energy*, vol. 111, pp. 474–486, 2018.

[13] M. A. R. Sheikh, E. Son, M. Kamiyama et al., "Sedimentation behavior of mixed solid particles," *Journal of Nuclear Science and Technology*, vol. 55, no. 6, pp. 623–633, 2018.

[14] B. Zhang, T. Harada, D. Hirahara et al., "Self-leveling onset criteria in debris beds," *Journal of Nuclear Science and Technology*, vol. 47, no. 4, pp. 384–395, 2010.

[15] T. Suzuki, K. Kamiyama, H. Yamano et al., "A scenario of core disruptive accident for Japan sodium-cooled fast reactor to achieve in-vessel retention," *Journal of Nuclear Science and Technology*, vol. 51, no. 4, pp. 493–513, 2014.

[16] J. C. Hesson, R. H. Sevy, and T. J. Marciniak, *Post-Accident Heat Removal in LMFBRS: In-Vessel Considerations*, Argonne National Laboratory, Lemont, IL, USA, 1971.

[17] J. D. Gabor, *Simulation Experiments for Internal Heat Generation*, Argonne National Laboratory, Lemont, IL, USA, 1974.

[18] D. Alvarez and M. Amblard, "Fuel leveling," in *Proceedings of the5th Information Exchange Meeting on Post Accident Debris Cooling*, Karlsruhe, Germany, July, 1982.

[19] E. Takasuo, "An experimental study of the coolability of debris beds with geometry variations," *Annals of Nuclear Energy*, vol. 92, pp. 251–261, 2016.

[20] Y. Chen and W. Ma, "Development and application of a surrogate model for quick estimation of ex-vessel debris bed coolability," *Nuclear Engineering and Design*, vol. 370, Article ID 110898, 2020.

[21] S. Basso, A. Konovalenko, S. Yakush, and P. Kudinov, "The effect of self-leveling on debris bed coolability under severe accident conditions," *Nuclear Engineering and Design*, vol. 305, pp. 246–259, 2016.

[22] S. Basso, A. Konovalenko, and P. Kudinov, "Effectiveness of the debris bed self-leveling under severe accident conditions," *Annals of Nuclear Energy*, vol. 95, pp. 75–85, 2016.

[23] A. Konovalenko, S. Basso, A. Karbojian, and P. Kudinov, "Experimental and analytical study of the particulate debris bed self-leveling," in *Proceeding of the 9th international topical meeting on nuclear thermal-hydraulics, operation and safety (NUTHOS-9)*, Kaohsiung, Taiwan, September, 2012.

[24] A. Konovalenko, S. Basso, P. Kudinov, and S. E. Yakush, "Experimental investigation of particulate debris spreading in a pool," *Nuclear Engineering and Design*, vol. 297, pp. 208–219, 2016.

[25] M. Hidaka, T. Fujii, and T. Sakai, "Improvement of molten core–concrete interaction model in debris spreading analysis module with consideration of concrete degradation by heat," *Journal of Nuclear Science and Technology*, vol. 53, no. 9, pp. 1260–1275, 2016.

[26] S. Yakush and P. Kudinov, "Simulation of ex-vessel debris bed formation and coolability in a LWR severe accident," in *Proceedings of the Implementation of Severe Accident Management Measures (ISAMM-2009)*, Böttstein, Switzerland, October, 2009.

[27] S. Yakush, P. Kudinov, and T. N. Dinh, "Multiscale simulations of self-organization phenomena in the formation and coolability of corium debris bed," in *Proceedings of the 13th International Topical Meeting On Nuclear Reactor Thermal Hydraulics (NURETH-13)*, Kanazawa, Japan, September 2009.

[28] W. Ma and T.-N. Dinh, "The effects of debris bed's prototypical characteristics on corium coolability in a LWR severe accident," *Nuclear Engineering and Design*, vol. 240, no. 3, pp. 598–608, 2010.

[29] M. Shamsuzzaman, B. Zhang, T. Horie et al., "Numerical study on sedimentation behavior of solid particles used as simulant fuel debris," *Journal of Nuclear Science and Technology*, vol. 51, no. 5, pp. 681–699, 2014.

[30] A. Jasmin Sudha, S. S. Murthy, M. Kumaresan, G. Lydia, B. K. Nashine, and P. Chellapandi, "Experimental analysis of heaping and self-levelling phenomena in core debris using lead spheres," *Experimental Thermal and Fluid Science*, vol. 68, pp. 239–246, 2015.

[31] S. Cheng, D. Hirahara, Y. Tanaka et al., "Experimental investigation of bubbling in particle beds with high solid holdup," *Experimental Thermal and Fluid Science*, vol. 35, no. 2, pp. 405–415, 2011.

[32] S. Cheng, H. Yamano, T. Suzuki et al., "Characteristics of self-leveling behavior of debris beds in a series of experiments," *Nuclear Engineering and Technology*, vol. 45, no. 3, pp. 323–334, 2013.

[33] S. Cheng, "Experimental studies and empirical model development for self-leveling behavior of debris bed," Doctoral Dissertation, Kyushu University, Fukuoka, Japan, 2011.

[34] S. Cheng, Y. Tanaka, Y. Gondai et al., "Experimental studies and empirical models for the transient self-leveling behavior in debris bed," *Journal of Nuclear Science and Technology*, vol. 48, no. 10, pp. 1327–1336, 2011.

[35] S. Cheng, H. Yamano, T. Suzuki et al., "Empirical correlations for predicting the self-leveling behavior of debris bed," *Nuclear Science and Techniques*, vol. 24, Article ID 010602, 2013.

[36] S. Cheng, H. Yamano, T. Suzuki et al., "An experimental investigation on self-leveling behavior of debris beds using gas-injection," *Experimental Thermal and Fluid Science*, vol. 48, pp. 110–121, 2013.

[37] S. Cheng, H. Tagami, H. Yamano et al., "Evaluation of debris bed self-leveling behavior: a simple empirical approach and its validations," *Annals of Nuclear Energy*, vol. 63, pp. 188–198, 2014.

[38] S. Cheng, H. Tagami, H. Yamano et al., "An investigation on debris bed self-leveling behavior with non-spherical particles," *Journal of Nuclear Science and Technology*, vol. 51, no. 9, pp. 1096–1106, 2014.

[39] S. Cheng, H. Tagami, H. Yamano et al., "Experimental study and empirical model development for self-leveling behavior of debris bed using gas-injection," *Mechanical Engineering Journal*, vol. 1, no. 4, 2014.

[40] C. Teng, B. Zhang, and J. Shan, "Study on relocation behavior of debris bed by improved bottom gas-injection experimental

method," *Nuclear Engineering and Technology*, vol. 53, no. 1, pp. 111–120, 2021.

[41] J. Harvey, K. S. Narayanan, S. K. Das et al., "Assessment of debris bed formation characteristics following core melt down scenario with simulant system," in *Proeedings of the 16th International Conference on Nuclear Engineering*, Orlando, Florida, USA, May 2008.

[42] L. Phan, P. Ngo, F. Matsuoka, R. Miura, T. Matsumoto, and K. Morita, "Experimental study on self-leveling behavior of binary-mixed particles in cylindrical bed using gas-injection method," in *Proeedings of the 12th International Topical Meeting on Reactor Thermal-Hydraulics, Operation, and Safety (NUTHOS-12)*, Qingdao, China, October 2018.

[43] L. H. S. Phan, P. M. Ngo, R. Miura et al., "Self-leveling behavior of mixed solid particles in cylindrical bed using gas-injection method," *Journal of Nuclear Science and Technology*, vol. 56, no. 1, pp. 111–122, 2019.

[44] H. Tagami, S. Cheng, Y. Tobita, and K. Morita, "Model for particle behavior in debris bed," *Nuclear Engineering and Design*, vol. 328, pp. 95–106, 2018.

[45] C. Teng, B. Zhang, J. Shan, X. Zhang, and Y. Cao, "Development of relocation model for debris particles in core disruptive accident analysis of sodium-cooled fast reactor," *Nuclear Engineering and Design*, vol. 368, Article ID 110795, 2020.

[46] K. Morita, T. Matsumoto, S. Nishi et al., "A new empirical model for self-leveling behavior of cylindrical particle beds," *Journal of Nuclear Science and Technology*, vol. 53, no. 5, pp. 713–725, 2016.

[47] M. Shamsuzzaman, T. Matsumoto, M. Kamiyama et al., "Experimental study on sedimentation behavior of core debris," in *Proeedings of the 9th Korea-Japan Symposium on Nuclear Thermal Hydraulics and Safety (NTHAS9)*, Buyeo, Korea, November 2014.

[48] K. Koide, K. Horibe, H. Kawabata, and S. Ito, "Critical gas velocity required for complete suspension of solid particles in solid-suspended bubble column with draught tube," *Journal of Chemical Engineering of Japan*, vol. 17, no. 4, pp. 368–374, 1984.

[49] K. Koide, T. Yasuda, S. Iwamoto, and E. Fukuda, "Critical gas velocity required for complete suspension of solid particles in solid-suspended bubble columns," *Journal of Chemical Engineering of Japan*, vol. 16, no. 1, pp. 7–12, 1983.

[50] M. Abraham, A. S. Khare, S. B. Sawant, and J. B. Joshi, "Critical gas velocity for suspension of solid particles in three-phase bubble columns," *Industrial and Engineering Chemistry Research*, vol. 31, no. 4, pp. 1136–1147, 1992.

[51] L.-S. Fan and C. Zhu, *Principles of Gas-Solid Flows*, Cambridge University Press, Cambridge, UK, 2005.

[52] S. Chiba, T. Chiba, A. W. Nienow, and H. Kobayashi, "The minimum fluidisation velocity, bed expansion and pressure-drop profile of binary particle mixtures," *Powder Technology*, vol. 22, no. 2, pp. 255–269, 1979.

[53] C. E. Agu, C. Pfeifer, and B. M. E. Moldestad, "Prediction of void fraction and minimum fluidization velocity of a binary mixture of particles: bed material and fuel particles," *Powder Technology*, vol. 349, pp. 99–107, 2019.

[54] R. Xu, S. Cheng, S. Li, and H. Cheng, "Knowledge from recent investigations on sloshing motion in a liquid pool with solid particles for severe accident analyses of sodium-cooled fast reactor," *Nuclear Engineering and Technology*, vol. 54, no. 2, pp. 589–600, 2022.

[55] S. Cheng and R. Xu, *Safety of Sodium-Cooled Fast Reactors: Particle-Bed-Related Phenomena in Severe Accidents*, Springer Nature Singapore, Beijing, China, 2021.

[56] S. Cheng, P. Gong, S. Wang et al., "Investigation of flow regime in debris bed formation behavior with nonspherical particles," *Nuclear Engineering and Technology*, vol. 50, no. 1, pp. 43–53, 2018.

[57] R. Xu, S. Cheng, Y. Xu, Y. Tan, and H. Zhang, "Investigations on flow-regime characteristics during debris bed formation behavior in sodium-cooled fast reactor by releasing high-temperature particles," *Nuclear Engineering and Design*, vol. 395, Article ID 111866, 2022.

[58] S. Cheng, L. He, F. Zhu et al., "Experimental study on flow regimes in debris bed formation behavior with mixed-size particles," *Annals of Nuclear Energy*, vol. 133, pp. 283–296, 2019.

[59] S. Cheng, W. Jin, Y. Qin, X. Zeng, and J. Wen, "Investigation of flow-regime characteristics in a sloshing pool with mixed-size solid particles," *Nuclear Engineering and Technology*, vol. 52, no. 5, pp. 925–936, 2020.

[60] S. Cheng, L. He, J. Wang, F. Zhu, and J. Cui, "An experimental study on debris bed formation behavior at bottom-heated boiling condition," *Annals of Nuclear Energy*, vol. 124, pp. 150–163, 2019.

[61] S. Cheng, J. Cui, Y. Qian et al., "An experimental investigation on flow-regime characteristics in debris bed formation behavior using gas-injection," *Annals of Nuclear Energy*, vol. 112, pp. 856–868, 2018.